Contract No:

This document was prepared in conjunction with work accomplished under Contract No. DE-AC09-08SR22470 with the U.S. Department of Energy (DOE) Office of Environmental Management (EM).

Disclaimer:

This work was prepared under an agreement with and funded by the U.S. Government. Neither the U. S. Government or its employees, nor any of its contractors, subcontractors or their employees, makes any express or implied:

1) warranty or assumes any legal liability for the accuracy, completeness, or for the use or results of such use of any information, product, or process disclosed; or
2) representation that such use or results of such use would not infringe privately owned rights; or
3) endorsement or recommendation of any specifically identified commercial product, process, or service.

Any views and opinions of authors expressed in this work do not necessarily state or reflect those of the United States Government, or its contractors, or subcontractors.

We put science to work.™

Savannah River National Laboratory ™

OPERATED BY SAVANNAH RIVER NUCLEAR SOLUTIONS

A U.S. DEPARTMENT OF ENERGY NATIONAL LABORATORY • SAVANNAH RIVER SITE • AIKEN, SC

Evaluation of the Current State of Knowledge for Thermolysis of Organics within SRS Waste Forming Volatile Organic Compounds (VOCs)

C. L. Crawford

S. D. Fink

C. A. Nash

J. M. Pareizs

SRNL.DOE.GOV

DISCLAIMER

Evaluation of the Current State of Knowledge for Thermolysis of Organics within SRS Waste Forming Volatile Organic Compounds (VOCs)

C. L. Crawford
S. D. Fink
C. A. Nash
J. M. Pareizs

February 2019

Savannah River
National Laboratory ™

OPERATED BY SAVANNAH RIVER NUCLEAR SOLUTIONS

REVIEWS AND APPROVALS

AUTHORS:

_____
C. L. Crawford, Advanced Characterization and Processing   Date

_____
S. D. Fink, Acting Director, Chemical Processing Technologies   Date

_____
C. A. Nash, Advanced Characterization and Processing   Date

_____
J. M. Pareizs, Process Technology Programs   Date

TECHNICAL REVIEW:

_____
A. L. Washington, Advanced Characterization and Processing, Reviewed per E7 2.60   Date

APPROVAL:

_____
B. J. Wiedenman, Manager   Date
Advanced Characterization and Processing

_____
F. M. Pennebaker, Manager   Date
Chemical Processing Technologies

_____
J. E. Occhipinti, Manager   Date
Waste Removal & Tank Closure, Tank Farm Facility Engineering

_____
E. J. Freed, Manager   Date
DWPF/Saltstone Facility Engineering

EXECUTIVE SUMMARY

The 2017 report *Flammable Gas Generation Mechanisms for High Level Liquid Waste Facilities*, X-ESR-G-00062 Rev. 1, assessing mechanisms for flammable gas generation acknowledged the presence of flammable organics, concluding that available data indicated their concentrations pose a minor contribution (e.g., <5%) to the composite lower flammable limit. Savannah River Remediation (SRR) chartered the Savannah River National Laboratory (SRNL) to perform a more detailed assessment of available and emerging data to assess the current state of knowledge for formation of Volatile Organic Compounds (VOCs) from thermolysis of organics in Savannah River Site (SRS) caustic tank waste.

Based on the assessment as detailed herein, SRNL concludes that sufficient evidence exists to demonstrate formation of methane, in addition to hydrogen, does occur during thermolysis of SRS high level waste containing organics under select conditions. This assessment cannot reliably quantify the amount of methane that forms. Nevertheless, the potential rates are sufficient – methane generation rates of approximately 30% and 100% those of hydrogen generation rates for Tank 38 radioactive waste and a high boiling point (HBP) simulant waste, respectively – to advise that ongoing program efforts be enhanced to include additional analysis for off-gas generation for concentration and screening measurements for other possible flammable species. The following paragraphs provide summary statements for the individual lines of inquiry that support this conclusion followed by a list of recommendations for the options of enhanced measurements.

- Review of recent SRS waste tank vapor sampling specific to Industrial Hygiene (IH) related hazardous components shows concentrations of numerous VOCs fell below the detection limits. These data have been compared to radiolytic Hydrogen Generation Rates (HGRs) from Concentration, Storage and Transfer Facility (CSTF) tanks to show that none of the VOCs at their detection limit concentrations would contribute more than 5% of the total hydrogen flammability per *Determination of the Flammability Ratio of Hydrogen Gas to Volatile Organic Carbons*, X-CLC-H-01225. In addition, the sampling program did not measure for the presence of methane, which is an expected species.

- Review of published data and reports from the Hanford Site yields the following key observations.

  o Testing with both simulated and actual Hanford Site high-level waste samples provides evidence of methane from thermolysis.
  o Testing shows the methane-to-hydrogen ratio increases with temperature, going from <0.05 at 60 °C, in the range of 0.21 to 0.42 for 90 °C and approaching values of between 0.5 (for 66 hour tests) and 1 (for 207 hour tests) at 120 °C. Ammonia concentrations relative to hydrogen increase from none detected at 60 °C to 90 °C, to ~3-4% at 120 °C with C_2 hydrocarbon (ethane, ethylene or acetylene) concentrations still less than 1% that of hydrogen.
  o HGRs decrease in going from 20% oxygenated to inert atmospheres for high Total Organic Carbon (TOC) Hanford samples, whereas methane rates are less affected, which may result in higher methane-to-hydrogen ratios in inert systems vs. the 20% oxygenated tests.
  o The Hanford Site high-level waste program uses a 10% of overall HGR as the bounding contribution for methane. Since the HGR is dependent on salt concentration, dose rate, temperature, TOC and aluminum concentrations, the methane generation rate fluctuates accordingly. This approach is in contrast to the fixed 5% of hydrogen lower flammability limit (LFL) that SRS uses for contribution from all VOCs.

- Given the recent and emerging SRNL experimental data from thermolysis of SRS simulated and actual waste reported in *Investigation of Thermolytic Hydrogen Generation Rate of Tank Farm Simulated and Actual Waste* (SRNL-STI-2017-00611, Rev. 0), it is demonstrated that VOC generation by thermolysis,

like that documented by Hanford studies cited in this report, could occur with SRS waste containing organics.

- The report on thermolysis testing of an actual SRS waste sample reported in *Investigation of Thermolytic Hydrogen Generation Rate of Tank Farm Simulated and Actual Waste* (SRNL-STI-2017-00611 Rev. 0) identified three unknown chromatograph peaks. Subsequent (and ongoing) analysis identified one peak as methane with the other two suspected as anomalous features. Preliminary estimates place the relative concentration of methane to hydrogen at ~30-35% for Tank 38 waste at boiling although the data is too sparse and too close to detection limits to provide a fully reliable value. The unknown chromatograph peak from simulant testing was also subsequently identified as methane. The simulant used conservative concentrations of multiple organics not likely to be present concurrently in a single waste feed. Preliminary estimates indicate equivalent concentrations of methane and hydrogen in the simulated waste tests that used high concentrations of the organics found in SRS waste.

- Presence of organo-mercury compounds may provide a route to methane formation, but confirmatory evidence is lacking for the waste matrix. Currently, the authors have not ascertained conclusive evidence of methane formation at SRS waste storage and processing conditions. The authors use recent data on stability of dimethyl mercury, which has been analyzed to be ~ 1 mg/L in some SRS CSTF tanks to provide an order of magnitude estimate of the potential generation rate for methane (e.g., methane generation rates of 9.1E-09 to 2.0E-06 ft^3/gal·hr in the temperature range of 39 to 170 °C in a High Level Waste (HLW) simulant) for comparison purposes. Unfortunately, the authors have not yet located sufficient data on methyl mercury, present at levels up to ~ 200 mg/L in SRS CSTF tanks, to allow estimating the methane generation rate for that compound in alkaline solution. However, an estimated methane generation in reagent water is provided (e.g., methane generation rates of 2.2E-07 to 4.5E-02 ft^3/gal·hr in the temperature range of 26 to 170 °C).

- Methane formation in the Bayer process from thermolysis tends to show a hydrogen-to-methane molar ratio of ≥75 (albeit at temperatures significantly higher than SRS waste processing conditions).

- Published studies of processing liquids obtained from the Bayer process cited in this report (from 2011 to 2016), albeit at more extreme conditions (175 °C to 275 °C), with a wide range of compounds, provide insight into the relative stability of classes of compounds toward hydrogen formation. By extrapolation and comparison to organics in SRS waste, antifoam is expected to show higher propensity for hydrogen (or flammable gas) formation. Ion exchange resins and solvents, in decreasing order, will likely yield lower quantities per unit mass of starting organic.

- Combined thermolysis and radiolysis studies for the cesium removal solvent suggest a potential methane-to-hydrogen ratio near ~0.24 with lesser amounts of other VOCs after long irradiation times. This magnitude agrees reasonably well with radiolysis data for PUREX solvent.

- Prior testing on off-gas production from thermolysis or radiolysis of antifoam does not provide insight into whether lighter VOCs formed. Preliminary findings from current SRNL HGR testing indicates that methane is produced at ~10X the rate as hydrogen from 100 °C thermolysis testing of the antifoam degradation product trimethylsilanol in a Tank 38 simulant.

- Decomposition of tributyl phosphates (TBP) and the degradation products in alkaline media is well studied. The authors found no literature evidence of methane generation from the TBP reaction system.

- Radiolytic decomposition of ion exchange resins to produce gaseous products in alkaline media is well studied. Degradation fragments from the organic backbone of resins exist in SRS waste. The authors found no literature evidence of VOC generation from thermolysis reactions involving these compounds. However, the absence of data may be a limitation of the prior testing focusing on hydrogen production and should not be construed as evidence that VOCs do not form.

Recommendations

1. Considering this assessment, SRNL recommends pursuing additional steps in ongoing and future experimental work to measure the presence of flammable VOCs in the thermolysis studies.

   a) In SRNL experiments, employ readily available gas analysis instrumentation (such as Fourier-transform Infrared (FTIR) spectroscopy coupled with Mass Spectroscopy (MS)) capable of quantifying simple VOCs such as methane, ethane/ethylene and other low carbon containing gaseous flammable hydrocarbons. Use this equipment first in experiments involving simulated waste to most quickly provide additional information on species present and approximate concentration ranges. Based on those findings, determine whether deployment with radioactive waste samples is warranted.

   b) Assess the option of altering the SRNL gas chromatograph (GC) protocols for (a) longer duration sampling capable of detecting at least ethane and possible C3 compounds on the second column used in the current GC system. In addition, consider (b) altering the carrier gas configuration to the second column within the GC to enhance sensitivity for analysis of these compounds. If the method appears viable, aggressively pursue implementation of these options in tests for both simulated and actual waste studies. Deploy these changes at the earliest practical date.

   c) Expand the available calibration gases for additional VOCs. By practical necessity and for expedient progress in understanding, these procurements should proceed in parallel with the previous two recommendations but not preclude development and testing of the alternate analytical protocols.

   d) Charter a Technical Agency to develop costs estimates and options for enhanced analytical methods for VOCs in the off-gas from future test programs and to enhance organic compound identification in high level waste samples.

2. A Technical Agency should conduct a review of prior sludge batch qualification off-gas analysis data for additional data related to presence of lighter VOCs other than the known ADPs. Similar reviews should occur of any archived data files for CSTF related off-gas studies that may also contain evidence of VOCs not previously identified.

3. If the review of prior sludge batch qualification off-gas analysis data shows presence of lighter VOCs, then SRR should consider requesting a Technical Agency to adopt similar expansion in analytical options for sludge batch qualification studies (i.e., actual waste sample testing) planned for the Defense Waste Processing Facility (DWPF).

4. SRR should reassess the current assumption that VOCs provide a bounding 5% contribution to composite flammable limit beyond that of hydrogen with emphasis on applications involving increased temperatures where thermolysis reactions could produce VOCs with generation rates of the same order of magnitude as HGRs produced by radiolysis or thermolysis.

5. SRR should consider including other VOCs such as methane, ethane and ethylene measurements in Industrial Hygiene sensitive volatile compounds from CSTF vapor sampling to provide information on these species with respect to possible flammability concerns.

6. SRR should consider requesting SRNL to perform thermolysis studies to investigate degradation of methylmercury to form hydrogen and VOCs in an alkaline aqueous waste matrix in addition to ongoing HGR studies involving prominent organics in SRS waste.

7. Revise the previous technical report on the thermolysis study of SRNL simulant and radioactive Tank 38 samples presented in *Investigation of Thermolytic Hydrogen Generation Rate of Tank Farm Simulated and Actual Waste* (SRNL-STI-2017-00611 Rev. 0) to include further treatment of the 'unknown' peaks identified in that work (that is presented in this study).

TABLE OF CONTENTS

LIST OF TABLES

LIST OF FIGURES

LIST OF ABBREVIATIONS

ADPs	Antifoam Degradation Products
CSSX	Caustic-Side Solvent Extraction
CSTF	Concentration, Storage and Transfer Facility
C_x hydrocarbons	Hydrocarbons with 'x' carbon atoms, where x = 2-6
DBP	Dibutyl Phosphate
DWPF	Defense Waste Processing Facility
EDTA	Ethylenediaminetetraacetic acid
FTIR	Fourier-transform Infrared
GC	Gas Chromatography
HBP	High Boiling Point
HEDTA	Hydroxyethylethylenediaminetriacetic acid
HEPA	High Efficiency Particulate Air
HGR	Hydrogen Generation Rate
HLW	High-level Waste
HMDSO	Hexamethyldisiloxane
IH	Industrial Hygiene
LOQ	Limit of Quantification
MCU	Modular Caustic-side Solvent Extraction Unit
MS	Mass Spectroscopy
NDMA	Nitrosodimethylamine
NFPA	National Fire Protection Association
NG-CSSX	Next Generation Caustic-Side Solvent Extraction
NIOSH	National Institute for Occupational Safety and Health
ORNL	Oak Ridge National Laboratory
PISA	Potential Inadequacy in the Safety Analysis
PUREX	Plutonium Uranium Redox Extraction
RF	Response Factor
SRNL	Savannah River National Laboratory
SRR	Savannah River Remediation
SVOA	Semi-Volatile Organic Analysis
TBP	Tri Butyl Phosphate
TIC	Total Inorganic Carbon
TMS	Trimethylsilanol
TOC	Total Organic Carbon
VOA	Volatile Organic Analysis
VOC	Volatile Organic Compounds
WAC	Waste Acceptance Characterization

1.0 Introduction

SRNL was tasked to evaluate the current state of knowledge of thermolysis of organics within SRS waste forming VOCs and to assess the need for measurement of flammable VOCs formed from thermolytic reactions for consideration in ongoing experimental planning.[1,2] These tasks satisfy Task 3 of the Task Technical Request (TTR) and deliverable number 7 in the TTR.[2]

This evaluation contains an extension of the discussion on VOCs contained in Section 3 (Radiolysis of Organics), Section 4 (Thermolysis Releasing Other Flammable Compounds) and Section 9 (Volatile Organic Compounds) of X-ESR-G-00062.[3] It provides additional discussion on unidentified gaseous species noted in Section 3.5 of recent Hydrogen Generation Rate (HGR) testing at SRNL on both simulants and radioactive samples in SRNL-STI-2017-00611.[4]

This evaluation draws on SRS sources of information pertaining to the organics present in SRS CSTF wastes,[5,6] previous work related to the SRS organics Potential Inadequacy in the Safety Analysis (PISA) from the early 2000 time period,[7, 8] as well as analogs from other industrial chemical processes.

The following areas of inquiry were pursued in this evaluation. These areas were pursued in parallel and each section is presented below in the listed order. Each section also contains key summaries listed in the highlight boxes.

- Review Sections 3, 4 and 9 of the Flammable Gas Generation Mechanisms report[3] with an emphasis on specifics of VOC species that were addressed.
- Examine recent (2017) SRS CSTF vapor sampling data.
- Present more detailed assessments of the Hanford HGR testing, with regards to VOCs, that was mentioned in Section 4 of X-ESR-G-00062.[3]
- Review and present additional information relative to 'unidentified' peaks noticed in the gas chromatography analysis from recent SRNL HGR testing that focused on hydrogen.[4]
- Assess existing literature data for organo-mercury compounds relevant to the flammability risks (i.e., as sources of either H_2 or flammable VOCs).
- Review results of work on the Bayer caustic aqueous process liquors involving high temperature decomposition of various organic components to form hydrogen.[9,10,11,12]
- Review results from thermolysis studies[58-66] performed on Caustic-Side Solvent Extraction (CSSX) Solvent and Next Generation Solvent.
- Review studies on antifoam degradation performed by SRNL and Vitreous State Laboratory (VSL).[68-75]
- Review studies on tributyl phosphate and the Plutonium Uranium Redox Extraction (PUREX) Solvent system degradation.[76-78]
- Review studies on Spent Ion Exchange Resin degradation.[79-81]

2.0 Reviews

2.1 Review of Flammable Gas Generation Mechanisms

The recent comprehensive report on Flammable Gas Generation Mechanisms focused on hydrogen generation from organics in SRS waste systems including the CSTF, DWPF and Saltstone Facility.[3] The PISAs for these facilities[13,14,15] and subsequent documents[16,17,18] that addressed inclusion of controls for the organic contribution due to radiolytic and thermolytic hydrogen generation focused on the flammable hydrogen gas product. Other flammable gas components with low carbon-number were discussed in the Flammable Gas Generation Mechanisms report.[3] Simple flammable compounds like methane, ethane,

propane and butane commonly formed from various radiolysis mechanisms were discussed in Section 3 (pages 45-46 and 49). Methane, ethane and ethylene from combined radiolysis/thermolysis testing of Hanford simulants and radioactive wastes were discussed in Section 4.[3]

Section 9 of the Flammable Gas Generation Mechanisms report[3], addressing Volatile Organic Compounds, does not mention formation of simple VOCs such as methane and ethane. These simple VOC species are also not specifically discussed in the 2002 PISA documentation.[7] The main VOCs discussed in the VOC Section 9[3] pertain to Antifoam Degradation Products (ADPs) and Isopar® L in the DWPF, and to the group of compounds that are controlled per the Saltstone Waste Acceptance Characterization (WAC)[19] (i.e., Isopar® L, benzene, and other organic components [i.e., butanol, tributyl phosphate (TBP) (which decomposes to butanol and dibutyl phosphate), isopropanol, methanol, and NORPAR 13]).

Section 9.4 of the Flammable Gas Generation Mechanisms report discusses the general status of potential VOCs in the CSTF by indicating that some waste streams may contain 'small' or 'trace' VOCs.[3] Based on historic assessments/analyses and the controls used on incoming waste to the CSTF, a contribution of 5% of the hydrogen LFL at 25°C for trace organics is considered a bounding value.

One reference from the PISA report that involved a 'Review of Miscellaneous Organic Compounds in the Tank Farm'[8] states the following.

> "*Many of the more volatile compounds transferred to the Tank Farms (e.g., toluene and ammonia) vaporize rapidly and if properly controlled by waste acceptance criteria would not be expected to be a problem. The production of volatile organic compounds by radiolysis of other organic compounds in the waste tanks is expected to be dwarfed by the radiolytic production of hydrogen, whose generation is well understood and documented. In general, radiolysis of organic materials follows a chain with the ultimate products being soluble organic acids and even the completely non-flammable carbon dioxide. Methane is not expected to be a primary radiolysis product of organics in the Tank Farm*".[8]

The review focused mainly on radiolysis of organics and also mentions 'chemical decomposition', but does not address thermolysis reactions occurring at elevated temperatures.[8]

The basis documents for defining organic components and explosive compounds in SRS waste do not mention the low carbon-number simple flammable VOCs as being original compounds present in SRS waste,[5] but do mention the possibility for formation of methane in addition to trimethyl amine and H_2 from Ion Exchange resin radiolytic degradation.[6] Hobbs addresses the possibility of 'other' flammable gases (relative to hydrogen and benzene) that conceivably are produced in SRS tank waste including ammonia, methane, ethane, ethylene and n-butanol.[6] However as pointed out in Section 9 of the Flammable Gas Generation Mechanisms report[3] and by Swingle in 1999,[8] the amount of ammonia and organic compounds in fresh waste is limited to reduce the possible formation of flammable ammonia and organic vapor mixtures via waste acceptance criteria for high level waste transfers to the F/H Tank Farms (pg. 14).[6] Previously reported analyses for samples obtained from SRS CSTF liquid waste indicate that ammonia and organic content of certain pump tanks and fresh waste

The recent assessment of mechanisms acknowledged the presence of flammable organics, concluding that available data indicated the concentrations pose a minor contribution (e.g., <5%) to the lower flammable limits.

receipt tanks is low and that no other volatile or semi-volatile organic compounds were detected.[6] Organics and ammonia are also limited in DWPF recycle streams that enter the F/H Tank Farms.[3,18,20]

2.2 Examination of SRS CSTF Hazardous Tank Vapors

An assessment of vapors from HLW tanks at the Hanford Site containing components potentially hazardous to nearby personnel from exposure indicated weaknesses in the understanding, monitoring and control of tank vapors.[21] As a result of that work a 'Vapor Review Team' was formed by Savannah River Remediation (SRR) personnel in December 2014 to review the Hanford Site report and compare the findings to the SRS CSTF. A subsequent 'SRR Gap Report' identified actions needed by SRR for the CSTF.[22] One of the outcomes of the Gap Report was a 'SRR Tank Vapor Action Plan'[23] which included planned vapor space analyses for SRS waste tanks. A subsequent SRS Tank Vapor Sampling Plan was issued.[24] Data from the sampling was used by SRR to examine flammability ratios of hydrogen to VOCs in late calendar year 2017.[25] A preliminary SRR Tank Vapor Report was issued in April of 2018 that described results from 30 tanks sampled from February 2017 through April 2018.[26] This hazardous tank vapors program focused on volatile components deemed potentially hazardous to personnel through exposure from an IH perspective (i.e., VOCs considered to form flammable mixtures in air were not explicitly included). The following information is derived from the references above.

- *Limitations of recent waste tank sampling show concentrations of numerous volatile organic compounds fell below the detection limits.*
- *Flammability ratio calculations for the VOCs and hydrogen indicate that the VOCs flammability contribution is less than 5%.*
- *Low carbon VOCs such as methane and ethane which could contribute to tank flammability were not included in the list of IH-related analytes.*

Table 2-1 shows some details of the Tank Vapor sampling plan.[24] Table 2-2 lists the Volatile Organic Compounds, Nitrosoamines, Total Mercury, Ammonia, and Oxides of Nitrogen on the compounds analysis list.[26]

Table 2-1. Tank Vapor Sampling Plan[24]

- ▪ **Collect head space vapor samples from all waste tanks, initially focusing on these types of evolutions:**

  - • **Waste Transfers**
  - • **Operation of Mixing Pumps**
  - • **Bulk waste removal or extended mixing pump operations (3 days of mixing)**
  - • **Ventilation-off condition**
  - • **Waste Transfer into evaporator drop tank**
  - • **Evaporator Recycle**

- ▪ **Vapor samples are collected by connecting downstream of the High Efficiency Particulate Air (HEPA)-VENT[TM] filter at the purge exhaust system Dispersed Oil Particulate test port.**

- ▪ **Sampling includes laboratory analysis for nitrosamines (Thermosorb/N[TM] media, 1.5-2 L/min flow rates) amines (Silica gel media, 2.5-3 L/min flow rates) and total organics (Coconut shell charcoal media, 0.15-0.2 L/min flow rates), all collected for 30-35 minutes sampling time. Various National Institute for Occupational Safety and Health (NIOSH) analytical methods were used to collect the vapor space data.[27]**

- ▪ **Direct read sampling for oxides of nitrogen, ammonia, and total mercury based on previous studies at SRR and reviews of Hanford Site sampling data.**

Table 2-2. IH Sensitive Compounds Analyzed in the SRR Tank Vapor Sampling Plan[26]

Volatile Organic Compounds

Acetone	Isopropyl Alcohol	N-Hexane
Benzene	Isopropylamine	Pentane
Carbon Tetrachloride	Methyl Amyl Ketone	Perchloroethylene
Cyclohexane	Methyl Ethyl Ketone	Styrene
Cyclohexylamine	Methyl Butyl Ketone	Toulene
Dimethylamine	Methyl Isoamyl Ketone	Trichloroethylene
Diethylamine	Methyl Isobutyl Ketone	Triethylamine
Ethanol	Methylamine	Xylene (Total)
Ethylamine	N-Butanol	M-Xylene
Ethylbenzene	B-Butyl Acetate	O-Xylene
Heptane	N-Butylamine	

Nitrosamines

N-Nitrosomethylethylamine	N-Nitrosodipropylamine (NDPA)	N-Nitrosopiperidine (NPip)
N-Nitrosodimethylamine (NDMA)	N-Nitrosodibutylamine (NDBA)	N-Nitrosomorpholine (NMor)
N-Nitrosodiethylamine (NDEA)	N-Nitrosopyrrolidine (NPyr)	

Total Mercury, Ammonia, and Oxides of Nitrogen

The Tank Vapor Report[26] indicates the following summary of data on the 30 sampled tanks:

1. All 30 tanks had VOCs and oxides of nitrogen below the limit of detection (LOD) except for Tank 48H in which benzene was detected at 0.5 mg/m^3.
2. Three waste tanks (30H, 39H and 43H) showed detectable ammonia as Tank 30H = 375 ug/m^3, Tank 39H = 1,500 ug/m^3 and Tank 43H = 187 to 1,400 ug/m^3.
3. Thirteen of the 30 waste tanks yielded positive detections for NDMA and one tank detected NPip.
4. Mercury was detected in all of the waste tanks except for Tank 45F and Tank 46F, which hold only saltcake waste.[28]

The flammability ratio calculation performed by SRR involving the VOC detection limits from tank vapor sampling and an average radiolytic hydrogen production rate indicates that the flammability contribution of the VOCs is less than 5% of the flammable contribution.[25] These results support use of the bounding 5% of hydrogen LFL for trace organic flammable gases as detailed in the SRR CSTF Flammability Control Program documentation.[29,30]

2.3 Examination of Hanford Site High-Level Waste Tanks HGR and VOCs

The complex chemistry associated with organics degradation from radiolysis and thermolysis in Hanford Site high-level waste was discussed in Section 4 of the Flammable Gas Generation Mechanism report.[3] Development of the HGR strategy for Hanford Site Tank Farm included testing of many simulant and actual radioactive samples.[31] Mass spectrometry was the main gas analysis technique used in these studies. Table 2-3 and Table 2-4 show summary molar gas generation rates for several radioactive tank samples as well as for a simulant of Tank AN-107 waste.[32] All data shown in Table 2-3 are for non-stirred radioactive

samples. The final column shows data for 'Total HCs' which is the sum of the C_2 hydrocarbons consisting of ethane, ethylene and acetylene and any other $>C_2$ hydrocarbons.[32] Data shown in Table 2-4 for the Tank AN-107 simulant includes effects of stirring on certain samples. The Tank AN-107 simulant contained a broad mixture of organic compounds (i.e., acetate, citrate, ethylenediaminetetraacetic acid (EDTA), formate, gluconate, glycolate, hydroxyethylethylenediaminetriacetic acid (HEDTA), iminodiacetate, nitriloacetate and oxalate) in the concentration range of 3E-03 to 0.25 M with a measured Total Organic Carbon (TOC) value of 21,300 mg/L. The data from Bryan et al.[32] shown in Table 2-3 and Table 2-4 are compiled in Table 2-5 and Table 2-6, respectively, to indicate molar $CH_4:H_2$ ratios from these tests.

Authors of the Hanford Site high-level waste study[32] concluded for the Table 2-3 data that for the higher TOC samples (Tank AN-102, AN-107 and U-106) an increase in oxygen from 0% to 20% caused a significant increase in HGR whereas going from 20% O_2 to 100% O_2 resulted in insignificant increase in HGR for all samples regardless of TOC content. They also assert that all levels of O_2 tested had little influence on the methane generation rate; however, oxygen increases the formation rate of Total HCs substantially, especially for the higher TOC wt % containing samples such as AN-102, AN-107 and U-106. Data in Table 2-5 for the inert and 20% O_2 testing may suggest that an inert atmosphere favors a higher molar methane-to-hydrogen ratio attributed to a lower HGR in inert atmosphere with insignificant change in methane generation rate. Data from Table 2-5 are plotted in Figure 2-1, Figure 2-2 and Figure 2-3 for the H_2 rate, the CH_4 rate and the $CH_4:H_2$ ratio, respectively. Hence, conditions that tend to consume oxygen in the liquid (e.g., long term static storage) may promote higher methane to hydrogen ratios for some organics.

All the methane to hydrogen ratios for Runs 1-13 from Table 2-6 for the simulant of Tank AN-107 are plotted in Figure 2-4. These data indicate $CH_4:H_2$ ratios in the range of 0 to 0.14 with all but one value being below 0.10, and the exception being a relatively high value of 0.45 for the stirred run performed at 0% O_2 and 90°C. The data of Figure 2-4 suggest an indeterminate relationship between oxygen content and methane-to-hydrogen ratio. Runs 4-5, 11-12 and 14-17 in Table 2-6 form the basis of a pH effect for hydrogen formation from thermolysis of Hanford Site high-level waste. These data are plotted in Figure 2-5.

Hydrogen formation rate significantly decreases in going from pH > 14 down to neutral pH of 7 and is non-detectable at pH 4. The opposite effect is seen for methane, which increases significantly in going from strong caustic of pH > 14 down to an acidic pH of 4. These data point to a gross effect in gas production with these simulants at the varied pH. However, the authors caution that both the neutral and acidic simulants used in that testing were derived from concentrated nitric acid addition to the original caustic simulants which could have chemically modified the simulant (i.e., gas evolution and solids formation upon acidification).

Table 2-3. Gas Generation Rates for 90°C Thermolysis Testing of Radioactive Hanford Site High-Level Waste Samples[32]

Hanford waste type	Cover gas	H_2 rate, mol/kg/d	std dev	CO_2 rate, mol/kg/d	std dev	CH_4 rate, mol/kg/d	std dev	N_2 rate, mol/kg/d	std dev	N_2O rate, mol/kg/d	std dev	Total HCs rate, mol/kg/d	std dev
AN-102	100% Ne	4.25E-05	7.90E-06	4.84E-05	9.83E-06	7.49E-06	1.12E-06	2.77E-04	5.54E-05	3.26E-04	6.09E-05	8.33E-06	6.92E-08
	20% O_2 in Ne	1.89E-04	1.56E-04	1.21E-04	1.24E-04	9.01E-06	8.48E-06	3.46E-03	1.82E-03	3.65E-03	3.25E-03	3.96E-05	1.38E-05
	100% O_2	1.14E-04	3.27E-05	2.33E-05	--	1.52E-06	8.01E-07	3.58E-03	2.38E-03	4.14E-03	3.95E-03	4.03E-05	3.12E-05
AN-106	100% Ne	8.48E-06	2.44E-06	1.70E-05	--	3.40E-06	--	2.54E-05	7.33E-06	2.55E-05	1.93E-05	--	--
	20% O_2 in Ne	1.65E-05	9.65E-06	3.54E-05	3.10E-05	4.45E-06	2.89E-06	1.63E-04	3.11E-04	1.55E-05	--	4.18E-06	4.69E-06
	100% O_2	1.71E-05	7.63E-06	4.48E-05	2.49E-05	--	--	1.84E-05	8.89E-06	--	--	5.47E-06	4.63E-06
AN-107	100% Ne	2.44E-06	1.15E-06	6.27E-05	8.11E-06	2.20E-05	1.49E-05	4.84E-04	4.81E-05	7.65E-04	9.14E-05	6.51E-06	5.90E-09
	20% O_2 in Ne	3.52E-05	2.10E-05	8.83E-05	5.13E-05	1.28E-05	9.87E-06	1.26E-02	1.10E-02	1.39E-02	1.29E-02	3.66E-05	3.62E-05
	100% O_2	3.17E-05	2.69E-05	3.88E-05	3.70E-05	5.39E-06	3.48E-06	1.67E-03	2.79E-04	9.41E-04	4.64E-04	2.02E-05	6.86E-06
AW-101	100% Ne	1.88E-04	6.92E-06	2.67E-05	1.86E-05	4.10E-05	2.86E-06	3.94E-04	5.24E-05	5.34E-04	2.38E-04	--	--
	20% O_2 in Ne	1.17E-04	6.95E-05	3.26E-05	3.39E-05	2.94E-05	4.70E-06	1.79E-04	2.55E-04	1.83E-05	5.69E-06	5.20E-06	9.56E-06
	100% O_2	1.88E-04	9.57E-05	3.66E-05	1.25E-05	2.81E-05	2.53E-06	1.07E-03	1.54E-03	--	--	--	--
U-106	100% Ne	5.21E-05	8.09E-06	3.31E-05	1.03E-05	6.09E-06	1.31E-06	1.49E-04	3.28E-05	2.49E-04	3.42E-05	6.07E-06	1.14E-06
	20% O_2 in Ne	2.10E-04	1.22E-04	9.85E-05	1.71E-05	7.03E-06	8.15E-06	5.59E-03	5.64E-03	9.50E-03	1.10E-02	6.10E-05	6.40E-05
	100% O_2	7.70E-05	3.24E-05	7.55E-05	8.72E-05	2.25E-06	--	3.13E-03	3.59E-03	2.90E-03	4.72E-03	4.54E-05	4.45E-05

Note: TOC levels (wt %) in these actual radioactive Hanford Site high-level waste samples: AN-102 = 2.02; AN-106 = 0.12; AN-107 = 1.09; AW-101 = 0.18; U-106 = 2.77; Test duration times in range of 17 to 286 hours.

Table 2-4. Gas Generation Rates for Thermolysis Tests Using Simulant AN-107[32]

Run	pH	% O_2	Temp, °C	H_2	CO_2	CO	CH_4	N_2	O_2	N_2O	NO_x	C_2H_x	>C_2 HCs	Sample ID
Standard AN-107 Simulant, Stirred Condition														
1	>14	0	90	3.22E-05	1.98E-05	6.44E-06	1.45E-05	--	-1.61E-06	5.63E-04	1.80E-03	--	--	WTP26-65-A
2	>14	20	60	1.22E-05	2.13E-05	2.37E-05	6.76E-07	--	(a)	4.73E-06	--	--	--	WTP26-50-A
3	>14	20	60	1.62E-05	4.16E-06	1.71E-05	--	--	-1.00E-02	6.66E-06	--	--	4.16E-07	WTP26-85-A
4	>14	20	90	1.37E-04	8.63E-06	1.44E-05	--	--	-1.79E-02	1.00E-04	--	--	--	WTP26-24-A
5	>14	20	90	1.63E-04	1.59E-05	4.81E-06	9.62E-07	--	-1.13E-02	8.51E-05	--	1.44E-06	--	WTP26-33-A
6	>14	20	120	4.02E-04	4.78E-05	--	6.87E-07	--	(a)	2.13E-03	1.92E-04	--	3.44E-07	WTP26-50-B
7	>14	20	120	5.61E-04	--	4.93E-06	--	--	(b)	2.83E-03	3.86E-04	--	--	WTP26-85-B
8	>14	100	90	1.11E-04	9.62E-06	1.50E-05	1.50E-06	--	-4.95E-02	3.27E-05	--	9.55E-07	2.05E-06	WTP26-70-A
9	>14	100	90	8.17E-05	6.41E-06	1.47E-05	7.05E-07	--	-4.37E-02	2.60E-05	--	5.13E-07	3.20E-06	WTP26-80-A
Standard AN-107 Simulant, Unstirred Condition														
10	>14	0	90	3.22E-05	1.46E-05	--	1.95E-06	--	-3.41E-06	6.72E-04	2.29E-04	--	--	WTP26-65-B
11	>14	20	90	2.42E-04	2.86E-05	--	--	--	-1.08E-02	3.34E-05	--	--	--	WTP26-24-B
12	>14	20	90	2.66E-04	1.86E-05	--	--	--	-7.25E-03	6.59E-05	--	--	--	WTP26-33-B
13	>14	100	90	1.27E-04	2.39E-05	--	--	1.77E-05	-9.32E-03	6.42E-05	--	--	4.43E-07	WTP26-70-B
Variable pH AN-107 Simulant, Stirred Condition, 90°C														
14	4.17	20	90	--	1.08E-02	--	2.39E-05	3.28E-03	-1.08E-02	7.49E-04	--	1.67E-05	8.53E-05	WTP26-43-A
15	4.62	20	90	--	1.83E-02	--	6.74E-05	3.15E-03	(b)	1.83E-03	3.30E-03	3.86E-05	7.72E-05	WTP26-90-A
16	7.35	20	90	6.56E-07	9.25E-03	--	8.20E-06	2.82E-04	-3.94E-03	1.30E-04	--	--	--	WTP26-90-B
17	7.55	20	90	1.60E-06	5.02E-03	--	1.52E-05	9.02E-04	-1.21E-02	2.70E-04	--	1.04E-05	4.55E-05	WTP26-43-B
Organic free AN-107 Simulant, Stirred Condition														
18	>14	0	90	2.16E-06	6.03E-05	--	--	--	--	1.29E-05	--	--	--	WTP26-75-A
19	>14	20	90	3.18E-06	--	--	1.77E-07	--	-2.17E-03	6.01E-06	--	--	--	WTP26-39-A
Organic free AN-107 Simulant, Unstirred Condition														
20	>14	0	90	1.60E-06	2.14E-05	--	--	--	--	1.23E-05	--	--	--	WTP26-75-B
21	>14	20	90	8.89E-06	2.57E-06	4.68E-06	--	--	-1.71E-03	3.04E-06	--	9.35E-07	--	WTP26-39-B

(a) The number cannot be determined due to amount of air contamination.
(b) All oxygen was consumed before the reaction terminated.

Note: TOC levels (mg/L) in the AN-107 with organics simulant = 21,300 mg/L; Calculated TOC for 'Organic free' AN-107 simulant = 0 mg/L; Test duration times in range of 40 to 99.5 hours.

Table 2-5. Ratios of CH$_4$:H$_2$ for Hanford Site High-Level Waste Radioactive 90 °C Thermolysis Tests[32] from Data Shown in Table 2-3

Hanford Site High-Level Waste Type	Cover Gas	H$_2$		CH$_4$		Molar Ratio CH$_4$:H$_2$
		mol/kg/d	ft^3/h/gal*	mol/kg/d	ft^3/h/gal*	
AN-102	100%Ne	4.25E-05	8.67E-06	7.49E-06	1.53E-06	0.18
	20%O$_2$/ Ne	1.89E-04	3.86E-05	9.01E-06	1.84E-06	0.05
	100%O$_2$	1.14E-04	2.33E-05	1.52E-06	3.10E-07	0.01
AN-106	100%Ne	8.48E-06	1.73E-06	3.40E-06	6.94E-07	0.4
	20%O$_2$/ Ne	1.65E-05	3.37E-06	4.45E-06	9.08E-07	0.27
	100%O$_2$	1.71E-05	3.49E-06	--	--	--
AN-107	100%Ne	2.44E-06	4.98E-07	2.20E-05	4.49E-06	9.02
	20%O$_2$/ Ne	3.52E-05	7.18E-06	1.28E-05	2.61E-06	0.36
	100%O$_2$	3.17E-05	6.47E-06	5.39E-06	1.10E-06	0.17
AW-101	100%Ne	1.88E-04	3.84E-05	4.10E-05	8.37E-06	0.22
	20%O$_2$/ Ne	1.17E-04	2.39E-05	2.94E-05	6.00E-06	0.25
	100%O$_2$	1.88E-04	3.84E-05	2.81E-05	5.73E-06	0.15
U-106	100%Ne	5.21E-05	1.06E-05	6.09E-06	1.24E-06	0.12
	20%O$_2$/ Ne	2.10E-04	4.28E-05	7.03E-06	1.43E-06	0.03
	100%O$_2$	7.70E-05	1.57E-05	2.25E-06	4.59E-07	0.03

*Rates calculated for 90 °C using assumed density of 1.23 kg/L
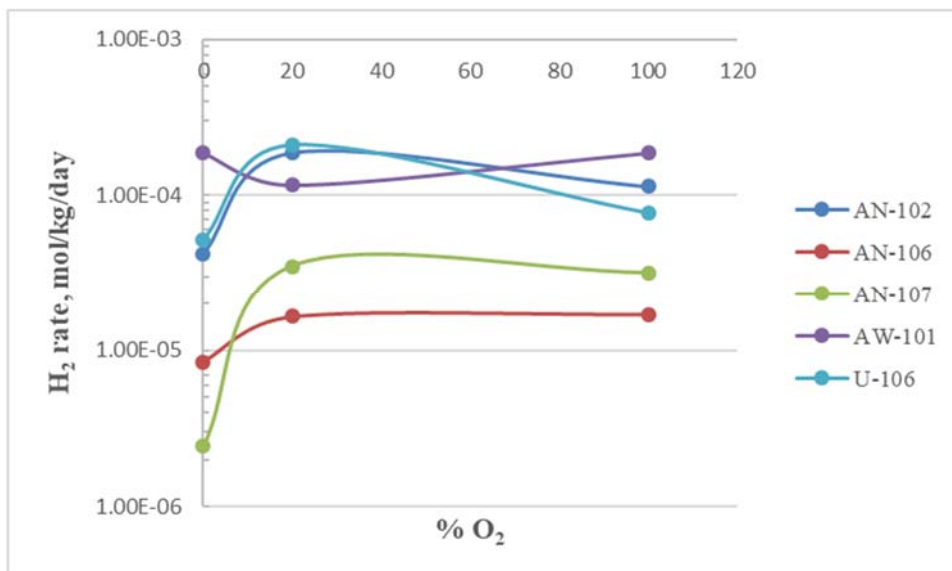
Figure 2-1. H$_2$ Rate as Function of %O$_2$ from 90 °C Hanford Site High-Level Waste Radioactive Sample Testing[32]
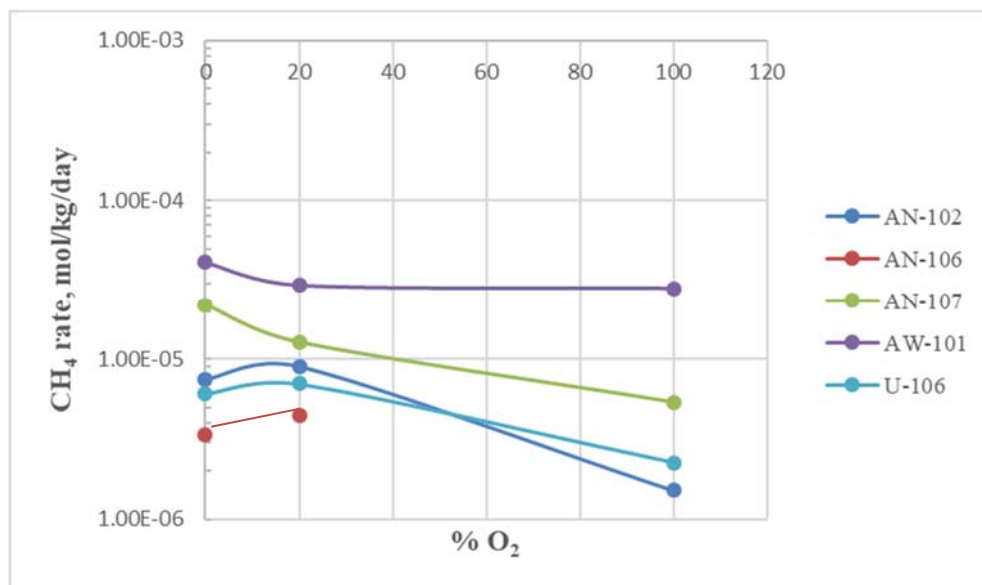
Figure 2-2. CH$_4$ Rate as Function of %O$_2$ from 90 °C Hanford Site High-Level Waste Radioactive Sample Testing[32]
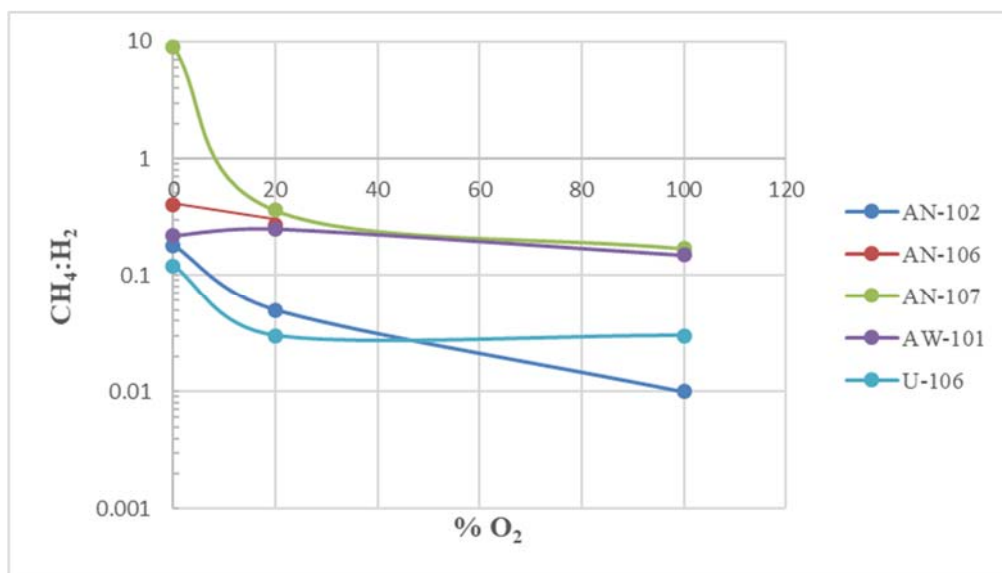
Figure 2-3. CH$_4$: H$_2$ Ratio as Function of %O$_2$ from 90 °C Hanford Radioactive Sample Testing[32]

Table 2-6. Ratios of CH$_4$:H$_2$ for Hanford Site High-Level Waste Simulant AN-107 Thermolysis Tests[32] from Data Shown in Table 2-4

Run*	pH	%O$_2$	Temp., °C	H$_2$ mol/kg/day	CH$_4$ mol/kg/day	Molar Ratio CH$_4$:H$_2$
1	>14	0	90	3.22E-05	1.45E-05	0.45
2	>14	20	60	1.22E-05	6.76E-07	0.06
3	>14	20	60	1.62E-05	--**	--
4	>14	20	90	1.37E-04	--**	--
5	>14	20	90	1.63E-04	9.62E-07	0.01
6	>14	20	120	4.02E-04	6.87E-07	<0.00
7	>14	20	120	5.61E-04	--**	--
8	>14	100	90	1.11E-04	1.50E-06	0.01
9	>14	100	90	8.17E-05	7.05E-07	0.01
10	>14	0	90	3.22E-05	1.95E-06	0.06
11	>14	20	90	2.42E-04	--**	--
12	>14	20	90	2.66E-04	--**	--
13	>14	100	90	1.27E-04	--**	--
14	4	20	90	--**	2.39E-05	infinite***
15	4	20	90	--**	6.74E-05	infinite***
16	7	20	90	6.56E-07	8.20E-06	12.50
17	7	20	90	1.60E-06	1.52E-05	9.50

* Runs 1-9 Stirred, Runs 10–13 Unstirred, and Runs 14-17 Stirred – these last four tests along with Runs 4 and 5 investigate gross pH effects.
** No hydrogen nor methane generation rates reported which suggests hydrogen and methane were below detection limit for these tests.
***No hydrogen was detected in these tests.
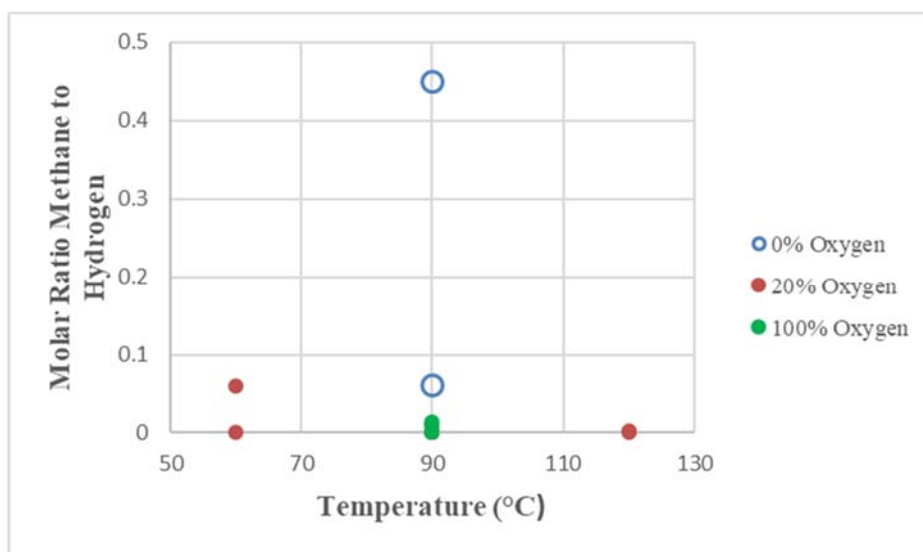
Figure 2-4. Molar Ratio of Methane to Hydrogen from Simulant AN-107 Tests[32] at pH > 14. The single relatively high data point at 0.45 for 0% oxygen derives from stirred condition test.
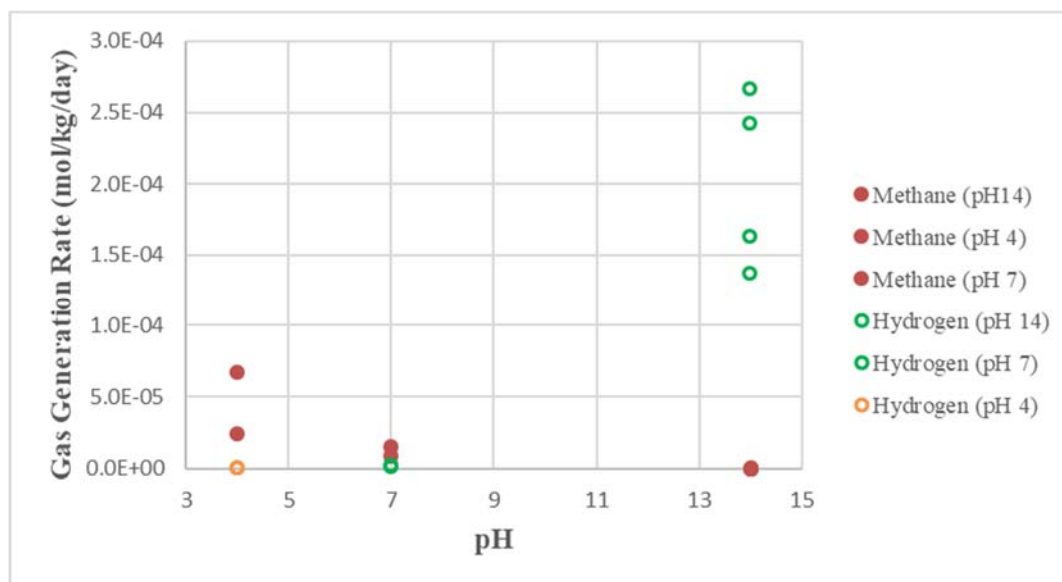
Figure 2-5. Gas Generation Rate from Simulant AN-107 Tests[32] from pH 4 to > 14 at 90 °C with 20% O_2. Higher HGR values at pH > 14 are for unstirred conditions and lower HGR values at pH > 14 are for stirred conditions.

Additional thermolysis testing has also been reported for actual radioactive waste tanks.[33] Table 2-7 shows molar gas generation results from heat treatment of waste from Hanford Site Tank U-103 and Table 2-8 gives the corresponding calculated molar ratios of the methane to hydrogen from the Tank U-103 data which was collected for periods up to 404 hours. The Tank U-103 radioactive sample studied consisted of saltcake with some liquid on the top and sludge on the bottom.[33] The Best-Basis Inventory data was cited

to estimate that this sample contained an overall TOC of 0.85 wt % with 0.25 wt % of that total attributed to carbon from oxalate.[33] Table 2-3 and Table 2-4 and Table 2-7 for the Hanford Site high-level waste data indicate that C_2 hydrocarbons were detected with various degrees of saturation, such as ethane (C_2H_6), ethylene (C_2H_4) and acetylene (C_2H_2). It was concluded from the Hanford Site high-level waste study that the C_2 hydrocarbons were produced at higher yield in the aged actual waste samples vs. the fresh Tank AN-107 simulant with added complexants and their remnants. Thus they attributed the C_2 hydrocarbon formation to 'other organic compounds in the (real) waste such as phosphate esters, hydrocarbons and their hydrolyzed and oxidized derivatives'.[32] Important conclusions of this data set, over the temperature range of 60 to 120 °C, are that the molar $CH_4:H_2$ ratio increases with increasing temperature, and that while the hydrogen thermolysis rate decreases in going from oxygenated to inert systems, the methane rate remains relatively steady.

The Hanford Site high-level waste data in Table 2-7 that is presented as relative concentrations in Table 2-8 roughly supports a conclusion of <5 vol % contribution from other flammable VOCs at lower temperature (i.e., 60 °C). However, from the plot shown in Figure 2-6, as temperature increases (120 °C), the concentrations of other species increase; methane can approach nearly equal concentrations to hydrogen for the longer term 207 hour tests and ammonia nears 5% relative concentration. Noteworthy is the observation that C_2 hydrocarbons remain below ~1% of the concentration of hydrogen at 120 °C. It is noted for the ammonia data shown in Table 2-7 that only the gaseous ammonia species is reported which does not include any ammonia dissolved in the liquid phase. A Hanford Site high-level waste study has shown that the solubility of ammonia in a Hanford Site SY-101 simulant can be several orders of magnitude higher than either H_2 or CH_4.[34]

Table 2-7. Gas Generation Rates from Thermal Treatment of Hanford Site High-Level Waste Tank U-103[33]

			60°C Gas Generation Rates, mol/kg/day						
Run	N_2	N_2O	H_2	$NH_3^{(a)}$	NO_x	CH_4	$C_2H_{2,4,or 6}$	Other HC$^{(b)}$	Total
1a	2.2E-6	6.5E-7	3.2E-6			7.0E-8	3.5E-8		6.1E-6
1b	2.5E-6	6.4E-7	3.2E-6			1.1E-7			6.5E-6
2a	2.5E-6	8.0E-7	3.7E-6			7.0E-8	3.5E-8		7.1E-6
2b	2.5E-6	8.1E-7	3.1E-6			1.1E-7			6.6E-6

			90°C Gas Generation Rates, mol/kg/day						
Run	N_2	N_2O	H_2	$NH_3^{(a)}$	NO_x	CH_4	$C_2H_{2,4,or 6}$	Other HC$^{(b)}$	Total
3a	1.3E-5	7.1E-6	2.7E-5			6.2E-6	2.1E-7	2.7E-8	5.4E-5
3b	1.4E-5	7.6E-6	1.4E-5			5.9E-6	9.5E-8	1.2E-7	4.1E-5
4a	8.7E-6	7.7E-6	2.1E-5			4.5E-6	1.7E-7	2.4E-8	4.2E-5
4b	8.0E-6	7.7E-6	9.3E-6		6.1E-7	2.9E-6	9.1E-8	1.1E-7	2.9E-5

			120°C Gas Generation Rates, mol/kg/day						
Run	N_2	N_2O	H_2	$NH_3^{(a)}$	NO_x	CH_4	$C_2H_{2,4,or 6}$	Other HC$^{(b)}$	Total
5a	2.8E-4	2.1E-4	5.0E-4		1.5E-6	2.7E-4	2.7E-6	2.7E-7	1.3E-3
5b	3.1E-4	4.8E-4	5.2E-4	2.0E-5		4.9E-4	1.2E-6	1.6E-7	1.8E-3
6a	3.3E-4	2.5E-4	5.6E-4	1.4E-5	2.5E-6	3.2E-4	3.0E-6	2.8E-7	1.5E-3
6b	3.1E-4	5.1E-4	5.6E-4	2.1E-5	1.3E-6	5.0E-4	1.3E-6	1.7E-7	1.9E-3

(a) Ammonia measurements are for gas phase only and do not include ammonia dissolved in the liquid phase.
(b) Hydrocarbons.

Note: Hanford Site high-level waste Tank U-103 cited as containing a total TOC of 0.85 wt %, with 0.25 wt % of the total assigned to oxalate; Times for Runs 1-4 = 311- 404 hours, Runs 5-6 = 66 – 307 hours

Table 2-8. Ratios of CH$_4$:H$_2$ for Thermal Treatment of Hanford Site High-Level Waste Tank U-103 Tests[33]

| Run/Time(h)	mol/kg/day					Ratio to Hydrogen		
	C$_2$H$_{2,4,\text{ or }6}$	H$_2$	CH$_4$	NH$_3$	Total	C$_2$H$_{2,4,\text{ or }6}$	CH$_4$	NH$_3$
60 °C								
1a / 404	3.50E-08	3.20E-06	7.00E-08	--	6.10E-06	0.01	0.02	--
1b / 311		3.20E-06	1.10E-07	--	6.50E-06	--	0.03	--
2a / 403	3.50E-08	3.70E-06	7.00E-08	--	7.10E-06	0.01	0.02	--
2b / 311		3.10E-06	1.10E-07	--	6.60E-06	--	0.04	--
90 °C								
3a / 403	2.10E-07	2.70E-05	6.20E-06	--	5.40E-05	0.01	0.23	--
3b / 311	9.50E-08	1.40E-05	5.90E-06	--	4.10E-05	0.01	0.42	--
4a / 404	1.70E-07	2.10E-05	4.50E-06	--	4.20E-05	0.01	0.21	--
4b / 311	9.10E-08	9.30E-06	2.90E-06	--	2.90E-05	0.01	0.31	--
120 °C								
5a / 66	2.70E-06	5.00E-04	2.74E-04	--	1.30E-03	0.01	0.55	--
5b / 307	1.20E-06	5.20E-04	4.90E-04	2.00E-05	1.80E-03	0.002	0.94	0.04
6a / 66	3.00E-06	5.60E-04	3.20E-04	1.40E-05	1.50E-03	0.01	0.57	0.03
6b / 307	1.30E-06	5.60E-04	5.00E-04	2.10E-05	1.90E-03	0.002	0.89	0.04
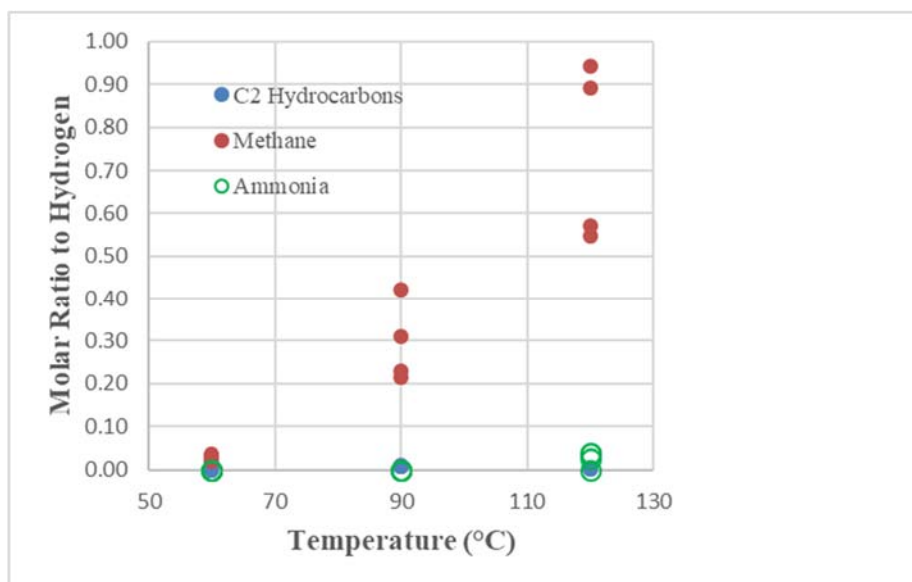
Figure 2-6. Molar Ratio of Product Gases Relative to Hydrogen from Hanford Site High-Level Waste Radioactive U-103 Testing.[33] Methane to Hydrogen molar ratios determined to be <0.05 at 60 °C for 311 to 403 hr tests; in the range of 0.21 to 0.42 at 90 °C for 311 to 403 hr tests; and for 120°C in the range of 0.55 to 0.57 for 66 hr tests and in the range of 0.89 to 0.94 for longer 207 hr tests.

A study involving thermolysis in the range of 60 to 120 °C on caustic simulants for durations of 2,000 to 5,000 hours containing HEDTA with inert Ar or mixed Ar/O_2 cover gases[35] also shows production of methane as shown in Table 2-9, with corresponding molar $CH_4:H_2$ ratios shown in the final data row of Table 2-10. At 60 °C no methane was detected with either cover gas. At 90 °C only the Ar/O_2 cover gas system showed detectable methane, with a $CH_4:H_2$ ratio of 0.13. All the 120 °C testing occurred with Ar cover gas and all of these systems show detectable methane with $CH_4:H_2$ ratios in the range of 0.29 to 0.66. Another screening test series conducted at 120 °C for shorter durations of 1,000 hours on various metal complexants in simulated waste shown in Table 2-11 indicates that molar methane to hydrogen ratios are only in the range of < 0.01 up to 0.4 as shown in Table 2-12.[35] An important data set in this test series for glycolate shows the molar $CH_4:H_2$ ratio is only 0.01. These data thus suggest that thermolysis of glycolate in SRS waste resulting from proposed alternative reduction processing in the DWPF should not produce significant amounts of methane relative to the higher levels of hydrogen expected.

Table 2-9. Gas Yields from Thermolysis Tests of the Reaction of HEDTA in Simulated Waste[35]

████████ Reaction of HEDTA in Simulated Waste at Different Temperatures.[1]						
Exp't	10B	16B	11B	17B	19B	12B
T/°C	60	60	90	90	120	120
Cover Gas	Ar	Ar\O$_2$	Ar	Ar\O$_2$	Ar	Ar
Time (h)	5036	3695	4942	3695	2038	2017 / 4921
HEDTA	98	93	36	88	<2	<2
HCOO$^-$	<1	13	107	25	139	152
(COO$^-$)$_2$	<2	<1	12	13	17	19
ED3A	<2	6	55	12	67	60
s-EDDA	<2	<2	6	~5	11	13
EDTA	<2	<2	<2	<2	~2	~2
AcO$^-$	<1	<1	~2	<1	3	4
H$_2$	0.6	0.9	3.9	11.7	6.3	6.4 / 11.3
O$_2$[2]	-	15	-	29	-	- / -
N$_2$	~3	~5	30	16	33	31 / 53
CH$_4$	<0.1	<0.1	0.5	<0.1	1.8	3.5 / 7.5
N$_2$O	<0.1	<0.1	24.5	1.0	36.1	31.9 / 27.1

[1]Unless otherwise stated, all products are indicated in moles per 100 moles of organic starting material. [2]Moles of O$_2$ *consumed* per 100 moles of HEDTA.

Table 2-10. Molar Ratios of CH$_4$:H$_2$ from Thermolysis Tests of HEDTA in Simulated Waste[35]

Experiment		10B		16B	11B		17B	19B	12B	
Temp. °C		60		60	90		90	120	120	
Cover		Ar		Ar/O$_2$	Ar		Ar/O$_2$	Ar	Ar	
Time(h)		5036		3695	4942		3695	2038	2017	4921
HEDTA %reacted		2		7	64		12	98	NA*	98
H$_2$**		0.6		0.9	3.9		11.7	6.3	6.4	11.3
CH$_4$**	<	0.1	<	0.1	0.5	<	0.1	1.8	3.5	7.5
Molar Ratio: CH$_4$:H$_2$	<	0.17	<	0.11	0.13	<	0.01	0.29	0.55	0.66

*Not Applicable; **moles of gas per 100 moles of organic starting material

Table 2-11. Gas Yields from Thermolysis Testing on Various Metal Complexants[35]

	Effect of Oxygen on the Reaction of Metal Complexants in Simulated Waste Solution (120° C, 1000 h)[1].								
Experiment	Atm	Starting Material	$HCOO^-$	$C_2O_4^-$	H_2	$O_2^{[2]}$	$N_2^{[3]}$	CH_4	N_2O
EDTA-5A	Ar	102	<1	<2	1.3	-	~4	<0.1	<0.1
Glycolate-14A	Ar	27.4	29.8	43.5	21.2	-	~7	0.3	14.6
HEDTA-22A	Ar	34.8	73.4	10.0	2.7	-	20	0.1	5.9
Glycine-1A	Ar	97	1.4	6.2	1.5	-	~4	<0.1	0.4
U-EDDA-1A	Ar	90[4]	7.0	<2	0.5	-	~7	0.1	0.5
S-EDDA-2A	Ar	86	1.9	<2	2.0	-	~10	0.8	0.5
IDA-1A	Ar	100	<1	<2	0.9	-	~3	<0.1	<0.1
NTA-2A	Ar	95	1.9	5.0	2.5	-	~11	0.2	<0.1
EDTA-6A	O_2	93	3.0	9.7	6.7	17	~3	0.1	<0.1
Glycolate-12A	O_2	7.8	34.4	48.3	26.8	25	~5	0.3	9.5
HEDTA-21A	O_2	30.4	79.9	10.5	2.6	24	~11	0.3	8.6
Glycine-1A	O_2	81	2.0	16.5	8.5	15	~3	<0.1	0.1
U-EDDA-2A	O_2	80[4]	17.8	4.8	2.2	23	13	<0.1	0.1
S-EDDA-1A	O_2	79	7	15.3	9.3	25	~6	0.1	0.3
IDA-2A	O_2	93	2.3	4.9	4.1	15	~8	<0.1	0.1
NTA-1A	O_2	92	3.3	11.6	6.7	22	~2	0.1	<0.1

[1]Unless otherwise stated, all percentages represent moles of product per 100 moles of organic starting material. [2]Amount of oxygen *consumed* per 100 moles of starting organic material. [3]A considerable deviation (~ 40% when %N_2 is < 10) can be expected for these values, due to air contamination. [4]Estimated values.

Table 2-12. Molar Ratios of Methane to Hydrogen from Thermolysis of Various Metal Complexants at 120 °C for 1,000 h from Data Shown in Table 2-11[35]

Complexant		Atm.		H_2*	CH_4*		CH_4:H_2
EDTA-5A		Ar		1.3	<0.1		<0.08
Glycolate-14A		Ar		21.2	0.3		0.01
HEDTA-22A		Ar		2.7	0.1		0.04
Glycine-1A		Ar		1.5	<0.1		<0.07
U-EDDA-1A		Ar		0.5	0.1		0.20
S-EDDA-2A		Ar		2	0.8		0.40
IDA-1A		Ar		0.9	<0.1		<0.11
NTA-2A		Ar		2.5	0.2		0.08
EDTA-6A		O_2		6.7	0.1		0.01
Glycolate-12A		O_2		26.8	0.3		0.01
HEDTA-21A		O_2		2.6	0.3		0.12
Glycine-1A		O_2		8.5	<0.1		<0.01
U-EDDA-1A		O_2		2.2	<0.1		<0.05
S-EDDA-1A		O_2		9.3	0.1		0.01
IDA-2A		O_2		4.1	<0.1		<0.02
NTA-1A		O_2		6.7	0.1		0.01

*moles of gas per 100 moles of organic starting material

Thermolysis testing results from Hanford Site high-level waste studies presented in this section include many samples with a wide range of TOC present (see footnotes to Table 2-3,[32] Table 2-4[32] and Table 2-7[33]). As noted in Appendix B of the Flammable Gas Generation Mechanisms report,[3] Hanford Site high-level waste samples used to develop their HGR data contain a wide range of TOC from 0.09 wt % up to 3.5 wt % with an average and standard deviation of 0.092 ± 1.10 wt %. SRS tank waste samples typically have lower maximum TOC values, especially when compared to the high organic containing complexant tanks at the Hanford Site, as cited in the Flammable Gas Generation Mechanisms report[3] with a SRS TOC maximum Tank 45 (0.79 wt %), Sludge Batch 9 slurry (0.1 wt %) and Tank 50 (nominally 0.04 wt %, with a Saltstone WAC limit of 0.4 wt %). However, regardless of the TOC levels in the Hanford Site high-level waste thermolysis studies cited in this section, the methane to hydrogen ratios appear to be persistent across the range of TOC present. As a result of the tests documented above pertaining to Hanford Site high-level waste radioactive and simulant samples and others documented by Hu,[31] the current Hanford Site Tank Farm strategy for HGR assumes that methane generation is 10% of the HGR model-calculated hydrogen generation rate from radiolysis, thermolysis and corrosion.[36] Table A-3 of Yarbrough indicates that the average Hanford Site Tank Farm temperatures including supernate and solids is 33 ± 15 °C, with a minimum and maximum listed as 16 °C and 80 °C, respectively.[36] Thus methane to hydrogen ratios shown for the lower temperature 60 °C data sets in Table 2-6, Table 2-8 and Table 2-10 support this strategy applied to all Hanford Site high-level waste tanks including those with relatively lower amounts of TOC such as Tanks AN-106, AW-101 and U-103.

As discussed in Section 4 of the Flammable Gas Generation Mechanisms report,[3] Stock reviewed the occurrence and chemistry of organic compounds in Hanford Site high-level waste tanks.[37] That work summarizes that volatile and semi-volatile organic compounds continuously evolve from the waste tanks at the Hanford Site. These species are formed in ongoing cascades of interdependent chemical and

radiolytic reactions of organic complexants, phosphate esters and hydrocarbons. Oxidation of the organics is cited as the principal pathway for their degradation. Quoting from the Executive Summary of that work:

" *Oxidation is initiated by radioactive decay processes, by thermal chemical reactions and by other chemical reactions that do not involve free radicals. The decay processes produce hydrogen atoms, hydroxyl radicals, nitric oxide and nitrogen dioxide. Similar radical reagents are also obtained by thermal reactions. These reactive substances transform the organic constituents into organic radicals. The radicals react with oxygen and the reactive radicals to give other organic intermediates and products that also react with ionic reagents to give other products. These reactions occur in parallel, and many different products are obtained……..*

Generally the organic intermediates formed in the initial reactions are more reactive than the compounds from which they were formed. Volatile organic compounds are obtained in both the beginning and later stages of the chemistry……….

*The chemistry and the propensity for volatile compounds formation become apparent when it is recognized that some complexants, phosphate esters and all the hydrocarbons degrade to produce methyl radical which can react with many waste constituent*s."

- *Methane / hydrogen ratio increases with temperature*
- *HGR decreases from 20% oxygenated to inerted systems for select cases, while methane remains relatively constant*
- *The Hanford program uses a 2X higher upper contribution for methane than SRS uses for contribution from all VOCs*
- *Testing with both simulant and actual waste samples at the Hanford Site provide evidence of methane from thermolysis*

Stock provides a suite of postulated chemical reactions involving the methyl radical with various 'reactive free radicals' ($OH\bullet$, $NO_2\bullet$, $CH_3\bullet$, $CH_3CH_2\bullet$) and Hg that could account for production of methane, ethane, dimethylmercury and other products (CH_3OO and CH_3NO). These reactions are shown in Table 2-13.

Table 2-13. Proposed Chemical Reactions in Hanford Waste as Presented by Stock[37]

$$CH_3 + OH \rightarrow CH_3OH$$
$$CH_3 + NO_2 \rightarrow CH_3ONO$$
$$CH_3 + NO_2 \rightarrow CH_3NO_2$$
$$CH_3 + CH_3 \rightarrow C_2H_6$$
$$CH_3 + CH_3CH_2 \rightarrow C_2H_4 + CH_4$$
$$2CH_3 + Hg \rightarrow Hg(CH_3)_2$$

$$CH_3 + O_2 \rightarrow CH_3OO$$
$$CH_3 + NO \rightarrow CH_3NO$$

The data and information cited in this section pertains directly to Hanford tank wastes. A generalized comparison of Hanford and SRS waste characteristics with emphasis on organics was documented in Appendix B of the Flammable Gas Generation Mechanisms report.[3] As concluded in that work and in the information cited regarding organic discharges to Hanford and SRS Tank Farms, it is expected that the Hanford Site could experience a much greater and more complex series of organic oxidation reactions and resulting hydrogen and organic by-product evolution from their complexant tank wastes. The metric ton quantities of organic complexants (including HEDTA ($C_{10}H_{18}N_2O_7$), Glycolate ($C_2H_3O_3^-$), Citrate ($C_6H_5O_7^{3-}$), and EDTA ($C_{10}H_{16}N_2O_8$)) comprise a large source of hydrocarbons that were not used at SRS.

However, even though significant differences exist in the history of processing and organics introduced into either Hanford or SRS Tank Farms, recent HGR testing at SRNL involving both a High Boiling Point (HBP) simulant and an actual radioactive Tank 38 sample have shown that indeed hydrogen is evolved from thermolysis reactions.[4]

2.4 <u>Investigation of VOCs from Recent SRNL Testing</u>

Since hydrogen generation from thermolysis of SRS Tank Waste and simulant samples has been verified,[4] it is prudent to consider the possibility of other VOCs produced from thermolysis of SRS Tank Waste. These VOCs could derive from reactions like those shown in Table 2-13. Potential source organics for the methyl radical formation include many SRS organic species as discussed and depicted in the Run Plan for simulant testing to screen and assess glycolate and CSTF waste tank organics at SRNL.[38] Figures 2, 3 and 4 from the simulant Run Plan show chemical structures of organics in SRS waste including antifoam degradation products, tributyl phosphate and degradation products, and ion exchange resins and proposed soluble fragments, respectively. Structures in these figures have methyl groups (-CH_3).

The recent testing detected three unidentified peaks in the off-gas from the Tank 38 experiment and one unidentified peak in the High Boiling Point (HBP) simulant testing.[4] The following analysis determined the gas eluting beyond nitrogen is very likely methane, while the two peaks seen in Tank 38 testing near hydrogen are artifacts of the gas chromatograph (GC). It should also be noted that more recent HGR testing involving a CSTF Tank 51 sample for Low Temperature Aluminum Dissolution (LTAD) indicates that "under all conditions of the LTAD tests, no clear methane peaks were detected, and the measured methane concentrations were therefore < 90 ppmv (less than the methane Limit of Quantification (LOQ))".[39] In addition, similar HGR testing of a CSTF Tank 22 sample was conducted[1] and no methane production was noted during testing to a limit of detection of ~ 1 ppmv. A technical report describing the results of the Tank 22 testing is forthcoming.

The GC instruments using molecular sieve columns for collection of data generated in past HGR testing of the Tank 38 waste conducted in the SRNL Shielded Cells Facility (SCF) and HBP simulant conducted at the Aiken County Technical Laboratory (ACTL) were optimized for hydrogen detection and used calibration gas that contained no VOCs. Even though hydrogen elutes quickly on the molecular sieve column of the GC, the data collection duration in the chromatograph was sufficient to capture peaks for some lower molecular weight compounds potentially present. After the original study, the Tank 38 waste and the HBP simulant GC data were compared to later chromatographs that used a calibration gas with methane.

In the Tank 38 testing, an unidentified peak was observed beyond nitrogen. Figure 2-7 shows a methane calibration gas superimposed upon a process sample from the Tank 38 testing. There is excellent agreement between this unknown peak and the methane peak; thus, this peak is very likely methane.

The time span between the original testing for hydrogen and the latter comparison to methane standards was four to five months; from August 2017 to January 2018 for Tank 38, and September 2017 to January

2018 for HBP. Because of the delay in calibration for methane, the results in this section are qualitative or, at best, semi-quantitative. The GC columns change over time, and a calibration performed months after the time data was acquired is not advisable. For example, elution times for peaks may shift slightly when there is an elapsed duration between measurements. Also, for the HBP testing, data collection time was set to 90 seconds, and methane eluted at the end of the plot; the GC method has been modified to have a longer (120 seconds) collection time for current experiments. Finally, in the Tank 38 testing, better separation between krypton and methane would be desirable; the method for future testing has been modified (i.e., column temperature pressure were lowered) to obtain better separation.

As discussed above, the areas for the unidentified peaks beyond nitrogen from the Tank 38 waste (and HBP simulant) testing were very likely methane. The respective calibration gas standards were used to estimate a methane concentration:

$$Methane\ Concentration = Methane\ Area\ in\ Gas\ Sample \times RF$$

where,

RF = Response Factor – methane concentration in a standard divided by the GC response (area).

Figure 2-8 shows hydrogen and methane concentration results for the Tank 38 testing, while Figure 2-13 shows results for the HBP simulant testing.

Specific data pertaining to methane for Tank 38 testing is as follows. For Tank 38 testing, methane RF was determined using a 500-ppm methane standard. The average area from 5 replicates was used to calculate an RF. Because the calibration gas measurements were made months after the experiment, the numerical results for methane should not be used as statistically qualified values. Nevertheless, observations can be made from the trends and relative results. Figure 2-8 shows methane does appear strongly correlated with hydrogen - peaking when hydrogen peaked, with highest concentrations observed during the higher temperatures of 110 °C and 100 °C with higher hydrogen concentrations. The Tank 38 data shows that the postulated methane concentrations are approximately one third of the hydrogen value (i.e., methane at 40 ppm and hydrogen at 120 ppm at 110 °C, and methane at 10 ppm and hydrogen at 30 ppm at 100 °C).

> *The recent report on thermolysis testing of an actual waste sample identified three unknown chromatograph peaks. Subsequent (and ongoing) analysis identifies one peak as methane with the other two suspected as anomalous features. Estimates place the relative concentration to hydrogen at ~30-35% from actual waste testing and as high as 100% for conservative simulant waste.*
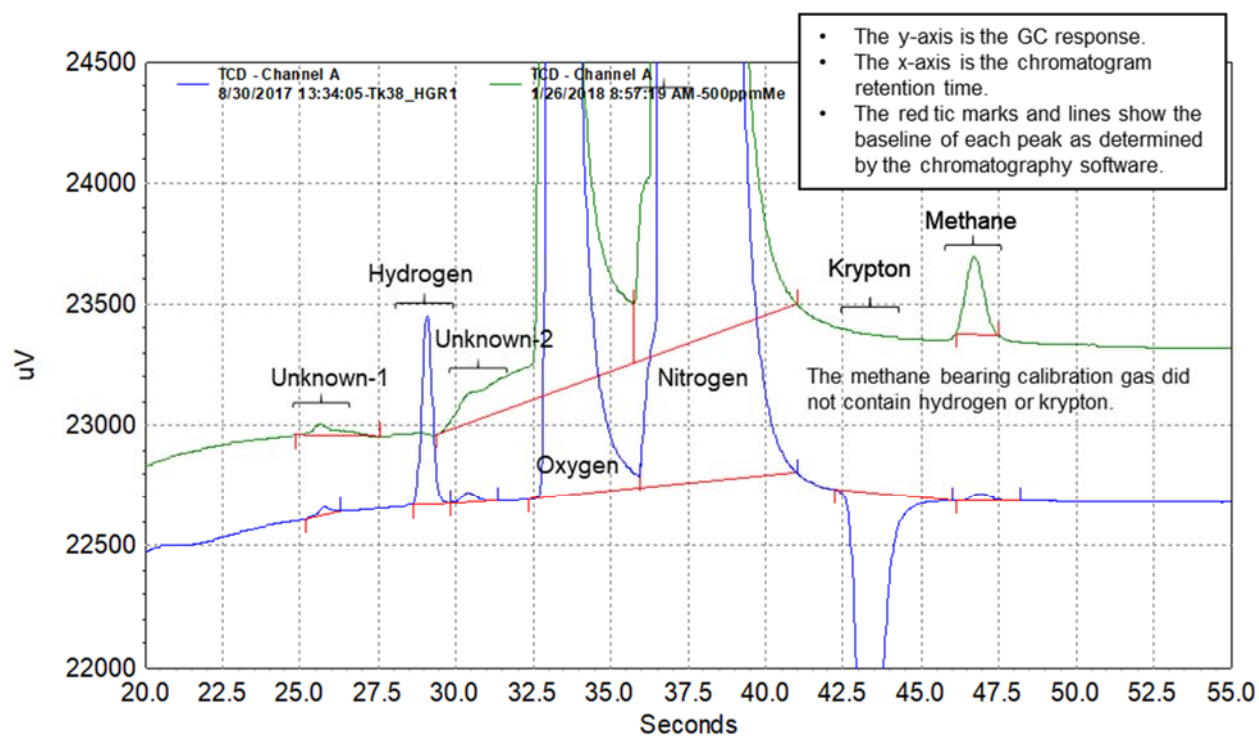
Figure 2-7. A 500 ppm Methane, Balance Air, Chromatogram Overlaid on a Tank 38 HGR Measurement Chromatogram
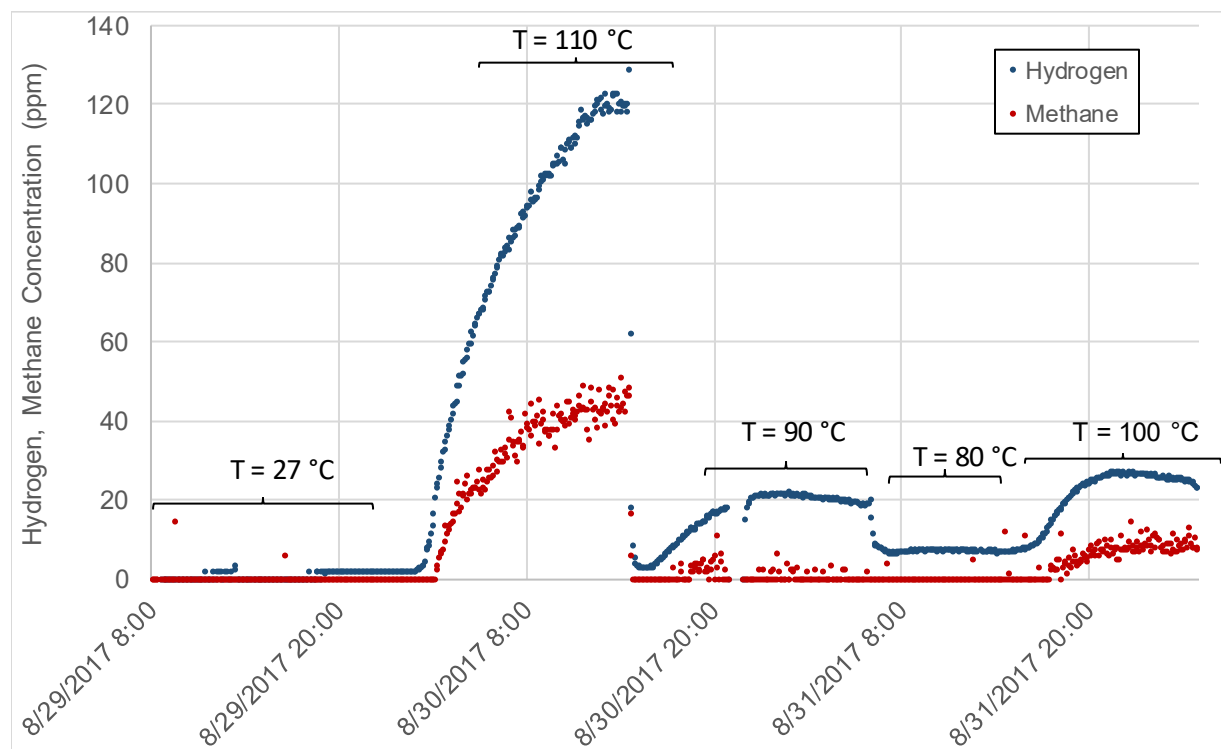

Figure 2-8. Concentrations for Hydrogen and Methane for Tank 38 Testing

Figure 2-7 also shows two other unidentified peaks on either side of the hydrogen peak (located at ~29 s). However, peaks at these elution times (i.e., ~26 s and ~31 s) appear in both the Tank 38 waste sample measurement and in the calibration standard measurement. Figure 2-9 shows a similar comparison but with a less concentrated (52 ppm) hydrogen standard collected during the original testing. Figure 2-10 shows the area measurements for the entire experiment with Tank 38 waste. Unlike the hydrogen and methane peaks, the calculated areas for these two unknowns seem largely invariant to temperature or other changes in conditions. Figure 2-11 shows area measurements for the two unknowns reporting in both blank air samples and for calibrations standards. Again, the concentrations (areas) seem largely invariant and equivalent to those from the Tank 38 experiment measurements. The consolidation of all these measurements strongly indicate that these two peaks are artifacts of the GC and piping system and not of a chemical compound evolving from the testing.
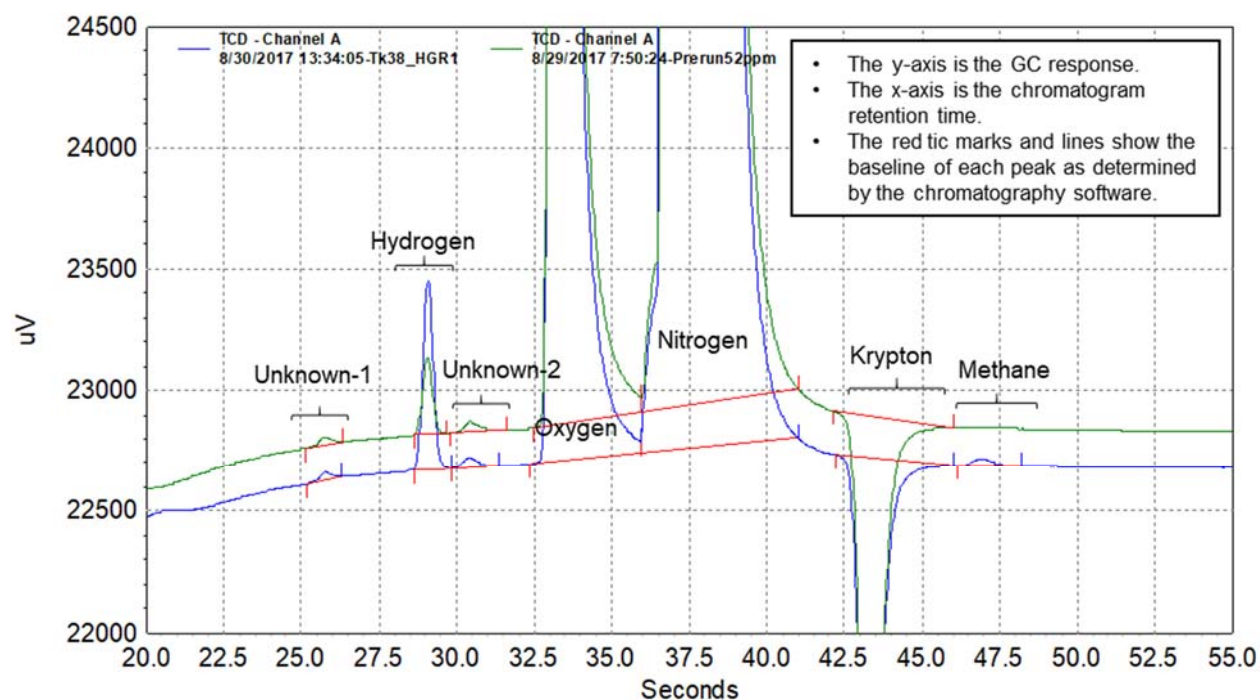

Figure 2-9. A 52 ppm Hydrogen, 0.5% Krypton, 20% Oxygen, Balance Nitrogen, Chromatogram Overlaid on a Tank 38 HGR Measurement Chromatogram
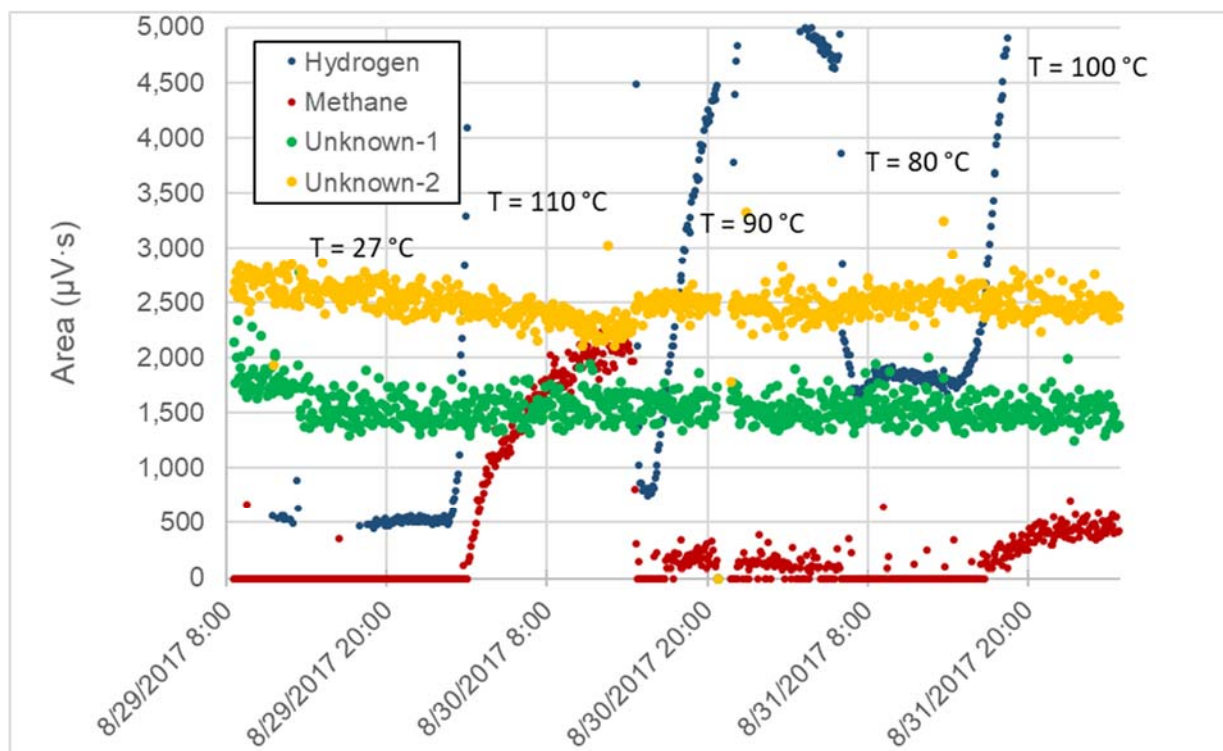
少

Figure 2-10. Unknown Peak Areas During Tank 38 experiments
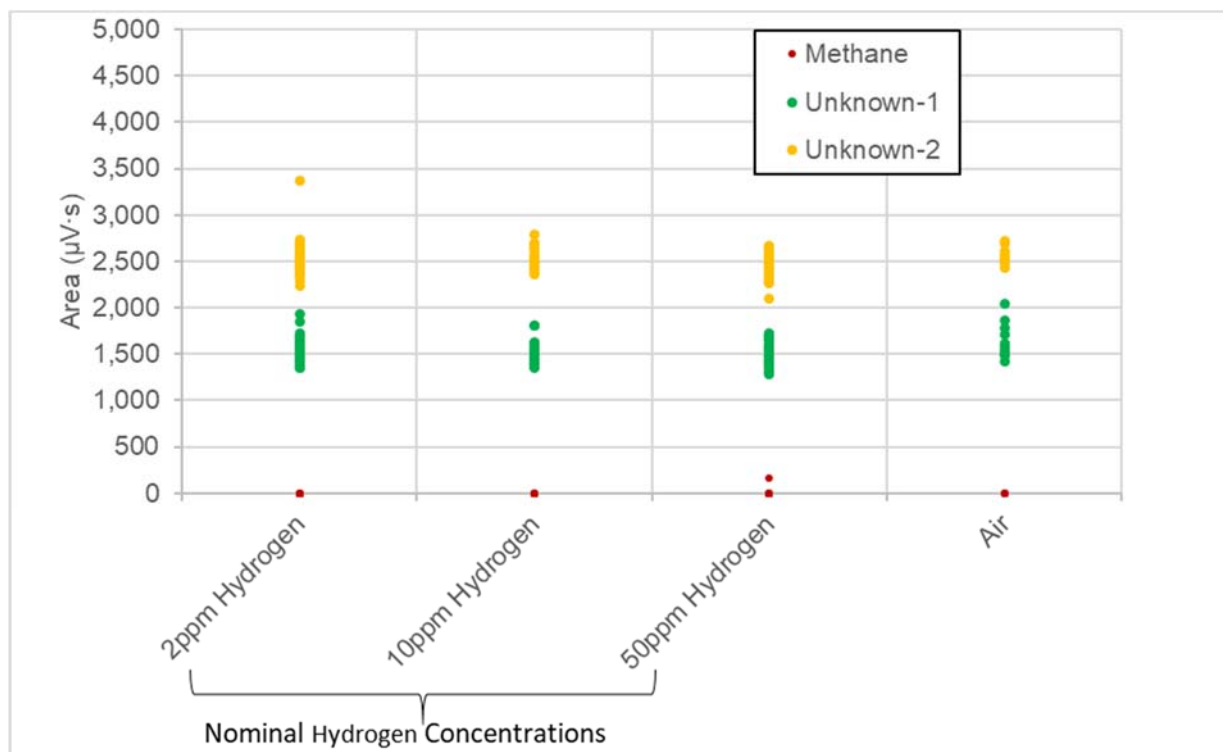

Figure 2-11. Unknown Peak Areas from Calibration Gases and Air

The testing with the HBP simulant served as an initial screening of the dominant organic constituents to provide an upper estimate of thermolysis risk or contribution. Hence, the testing combined all the various organics into a single series of (intended) "isothermal" tests. Concentrations used for each constituent represent near bounding values. Hence, the testing is "ultra-conservative" and "non-representative" for specific operations in CSTF in the sense that the total organic loading is falsely elevated, and a mixture of organics is present that will not occur under planned operations. Another differentiating feature is that the organics were added "freshly" to the waste, some at elevated temperature, and hence do not mimic the radiolytic and chemical degradation history appropriate for several of the species. The presumption is that some of the fresh compounds will be less stable than those that degrade over time in the radiolytic field or the high concentration caustic waste. The organics used in the SRNL HBP simulant included:[4]

- 3000 mg/L formate (added as sodium formate, above maximum concentration in SRS waste),
- 88 mg/L oxalate (added as sodium oxalate, near solubility limit at Tank Farm conditions),
- 1000 mg/L ion exchange resin (added as IONAC A641),
- 1000 mg/L antifoam (added as Antifoam 747),
- 1000 mg/L tributyl phosphate (near maximum concentration in SRS waste), and
- 78 mg/L Modular Caustic-Side Solvent Extraction Unit (MCU) solvent (at Waste Acceptance Criteria limit).

The measured TOC in the liquid phase for this simulant ranged from 0.088 wt % at 75 ºC up to 0.12 wt % at 140 ºC.[4]

Specific data pertaining to methane for HBP simulant testing is as follows. Figure 2-12 displays a chromatograph from Column A from the original HBP simulant tests with a later methane-bearing calibration gas chromatograph. As can be seen in Figure 2-12, all peaks have shifted slightly to the right (i.e., to later elution times) with the calibration gas with respect to the process sample collected several months earlier. The "unknown" peak at around 90 seconds in the HBP chromatogram corresponds very well with the methane peak in the calibration gas. This peak is the same one identified in the test report Figure 3-31.[4] Because the unknown peak aligns with methane in the calibration gas in both the Tank 38 and HBP testing, and methane has been identified in Hanford testing, it is very likely this unknown peak is indeed methane.
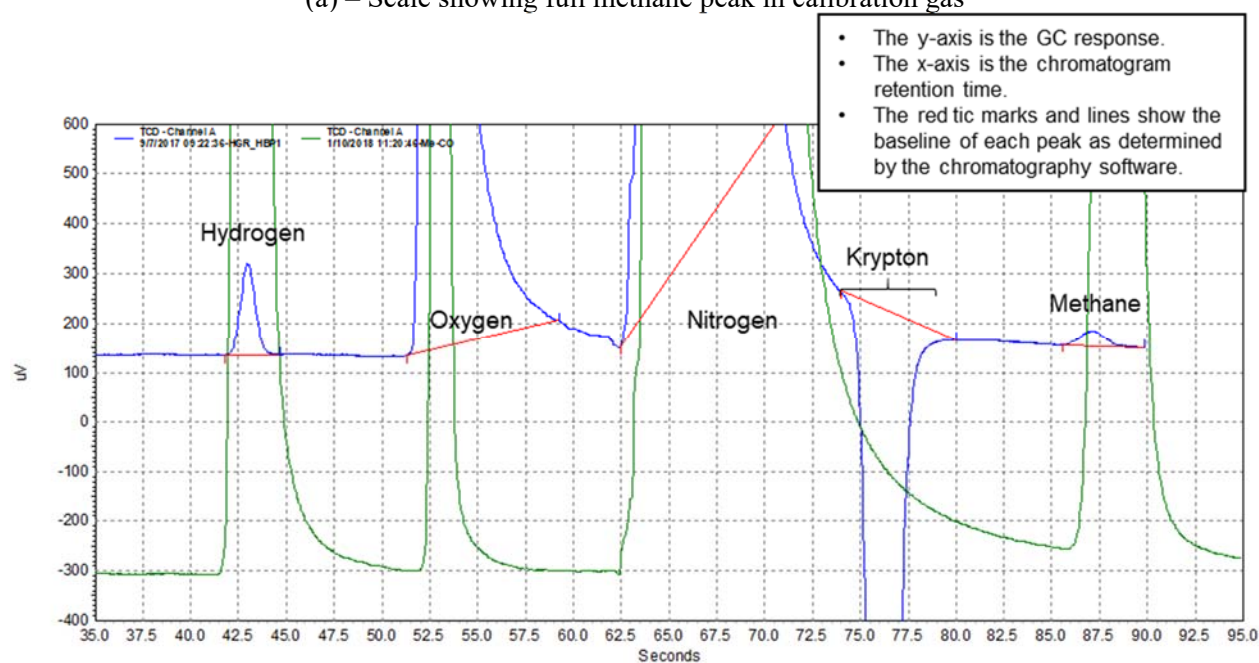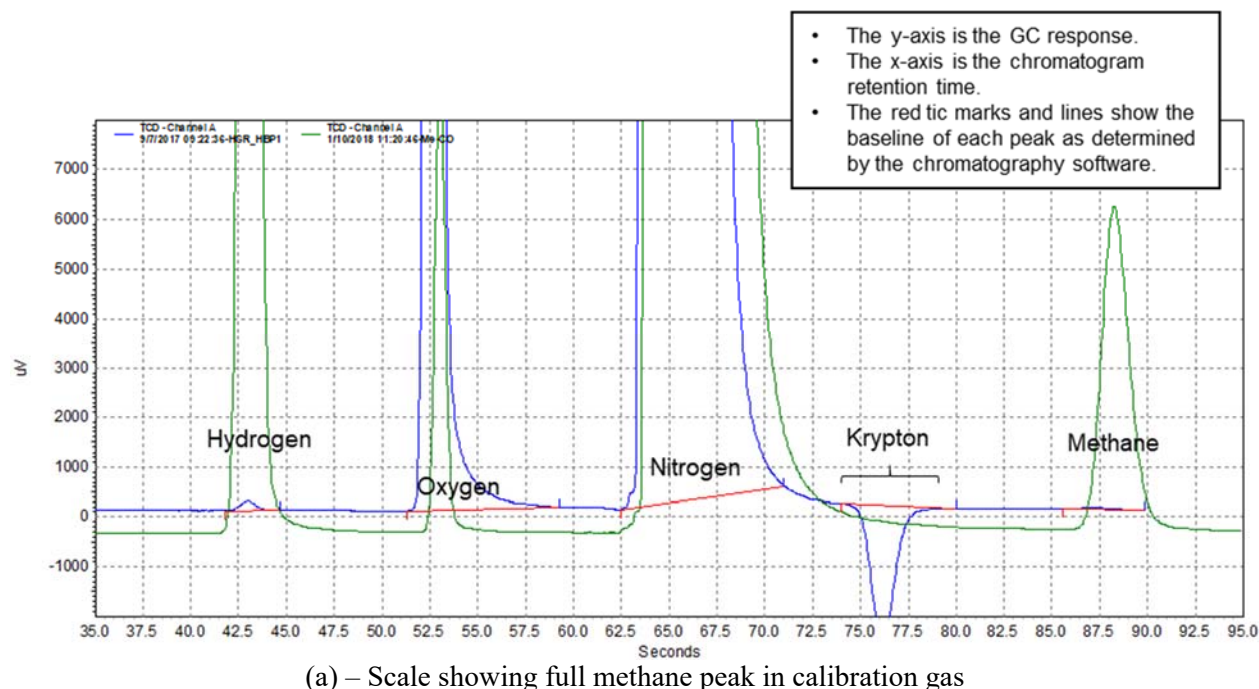
(a) – Scale showing full methane peak in calibration gas

(b) – Magnified to show hydrogen and methane peaks in HBP sample

Figure 2-12. A 1% Methane, 1% Hydrogen, 1% Oxygen, 1% Carbon Monoxide, Balance Nitrogen Chromatogram Overlaid on a HBP Testing Chromatogram

For the HBP simulant testing, methane concentration was estimated using a 1,000-ppm methane standard. The average area from 8 replicates was used to calculate an RF.   Because the calibration gas measurements occurred months after the experiment with longer data collection times (i.e., methane during the testing eluted at the very end of each GC analysis), the numerical results should be used with caution. Even so, methane was produced in similar quantities relative to hydrogen.

The time regimes A through G in Figure 2-13 correspond to the plot shown in Figure 3-10 of the original report for the HBP.[4] There was a relatively constant methane concentration at 140 °C concurrent with a decreasing hydrogen concentration.   The nearly constant methane concentration trend matches the expectation for isothermal thermolysis production when the parent reactant (presumably organic) is present in excess. In contrast, the declining hydrogen concentration is more typical of a parent species present in limited quantities and rapidly reacting at the elevated temperature. (Although it is not possible to link the behavior with specific organics in the broad mixture and limited test data, pretest expectations are that the ion exchange resin will have higher relative stability and the antifoam will undergo rapid degradation.) In any case, the differing concentration trends may reflect different reaction schemes for hydrogen and methane. One caveat to mention in the HBP testing is that the highest temperature was tested first, followed by lower temperatures, thus some of the original organic could have been consumed and biased the remaining lower temperatures tested. However, this testing scheme should represent a bounding scenario of tank waste behavior after evaporation. Further thermolysis HGR testing involving the reverse of this temperature progression (i.e., from lower temperatures up to the boiling temperature) would be required to test tank waste behavior leading up to evaporation.

At 100 °C and at 75 °C the methane concentration fell at or below the LOQ. In contrast to the behavior at boiling conditions, the methane and hydrogen concentrations curves are highly correlated, and the methane concentration matches or slightly exceeds that of hydrogen. The shift in methane trend from constant at the higher temperature to varying at the lower temperature may suggest that the reaction occurring at boiling ceases, or is greatly diminished, at the lower temperature while a lower yield second reaction, obscured at the elevated temperature, continues at all three temperatures.
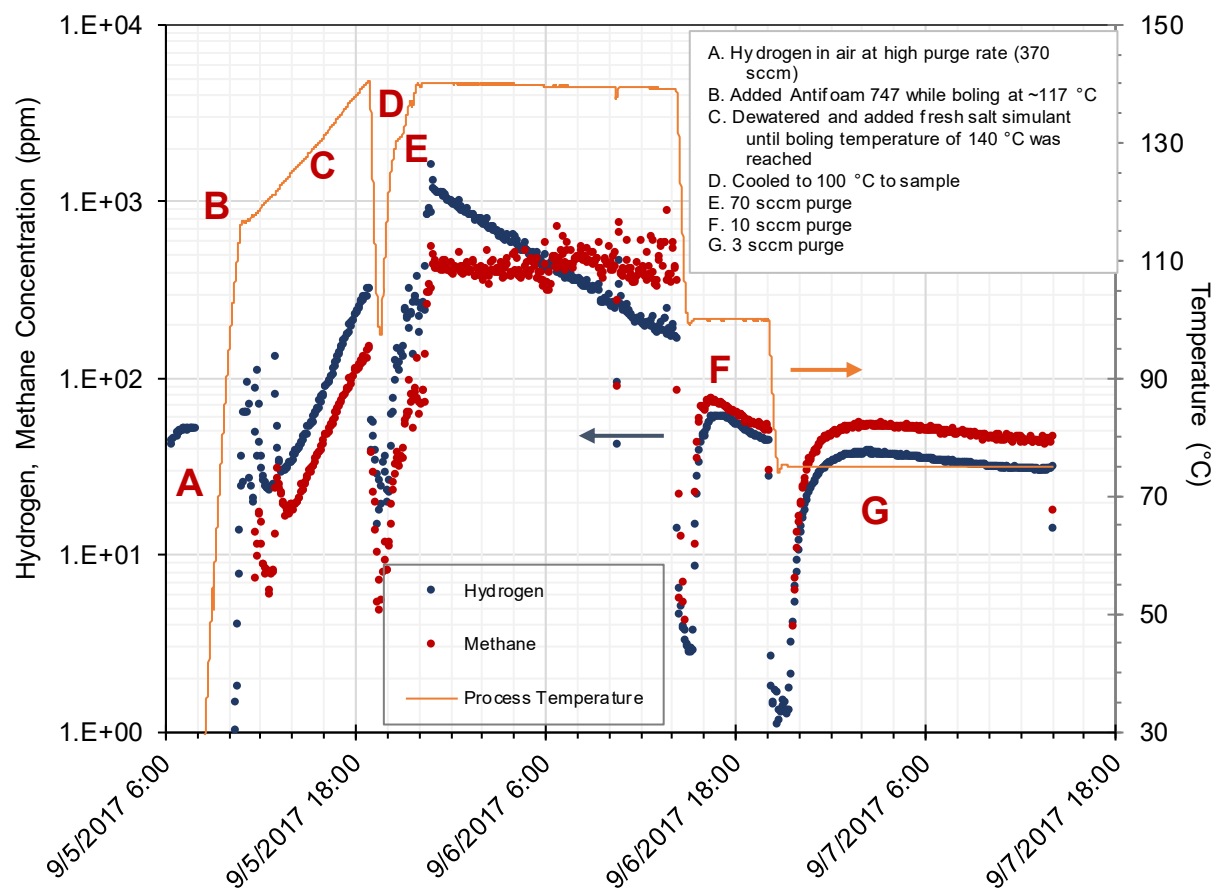
Figure 2-13. Concentrations for Hydrogen and Unidentified Peak as Methane for HBP Testing
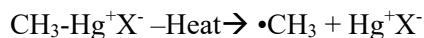
2.5 Organo-Mercury Compounds

Organo-mercury compounds have been identified in SRS Tank Farm samples in recent studies.[40,41,42,43,44] Methyl mercury is confirmed present in Tank 50 supernate at concentrations up to 60 mg/L.[42] Both dimethyl mercury and ethyl mercury are typically below 1 mg/L; for instance, the 3rd quarter 2017 Tank 50 supernate showed < 0.17 mg/L Hg as ethyl mercury and 0.062 mg/L Hg as dimethyl mercury.[40] Methyl mercury has been measured in the range of 2.5 to 200 mg/L in samples from the SRS 2H Evaporator tanks with detectable dimethyl mercury values in the range of 8.9E-04 to 0.6 mg/L.[42,44] Formation of dimethyl mercury in simulated SRS waste tank solutions has been studied in the temperature range of 40 °C to 80 °C.[45] One of the findings of that work indicates that alkaline waste solutions containing organics such as acetate and antifoam agent polydimethylsiloxane can rapidly methylate all of the Hg(II) present in solution to methyl mercury, and then, more slowly over time generate dimethyl mercury.

Soluble organo-mercury(II) species in aqueous solutions (RHgX and R_2Hg) are light sensitive, radiation sensitive and temperature sensitive to decomposition producing free radicals.[46] Analytical samples collected from SRS Tank Farm waste samples are routinely stored in shrouded containers and refrigerated at ~ 4°C in preparation for offsite shipment as concentrated hydrochloric acid preserved samples for analysis.[47] Samples for methyl mercury analysis are refrigerated and acidified with 0.4% HCl and kept in
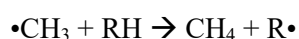
poly bottles in the dark to avoid photodegradation. For volatile species Hg^0 and dimethyl mercury analysis, samples are collected in zero-headspace shrouded glass bottles with Teflon-lined caps. It is noted that these volatile species are lost rapidly from Teflon and polyethylene bottles. Light sensitivity, photolytic degradation, was considered within the waste tank and reasoned as not a significant factor (see Section 6 and Appendix A.6 of the Flammable Gas Generation Mechanisms report[3]). Organo-mercury compounds in natural environments like lakes, sediments and oceans are well studied due to the varied chemistry and the toxicity of mercury compounds to humans.[48,49] A 2010 review indicates that elemental Hg(0) constitutes >99% of the total Hg in the atmosphere.[50] Bio/geochemical transformations can lead to Hg species in oxidation states of +I and +II. The Hg(I) compounds are mainly insoluble (i.e., soils and sediments) while Hg(II) complexes with inorganic and organic species to form compounds such as methyl mercury ($MeHg^+X^-$, where X^- represents any anion species) and dimethyl mercury ($(CH_3)_2Hg$). Dissolved organic matter (DOM), which is ubiquitous in aquatic environments, is known to bind trace metals strongly and affect their speciation, solubility, mobility and toxicity.[51] Formation of the organo-mercury species typically occurs through 'biomethylation'. These reactions are reversible with 'demethylation' that can also be driven by microorganisms to produce methane[48] or through photolytic decomposition.[49] One study performed on the species-specific degradation behavior of methyl mercury and ethyl mercury under microwave irradiation for up to 10 min and 160 W indicates the methyl mercury stability (practically no degradation) is much greater than ethyl mercury which showed significant analyte loss even at 2 min microwave at low 40 W power.[52] These tests were performed in 4.5 M methanolic NaOH solution to simulate caustic digestion commonly used for liberating mercury species from solid samples. The authors attribute their observations of methyl mercury stability to the stronger C-Hg bond strength vs. that bond strength in ethyl mercury species.

Presence of organo-mercury compounds may provide a route to methane formation from thermolysis but confirmatory evidence is lacking for waste matrix.

One can postulate chemical mechanisms under radiolysis or thermolysis for organo-mercury species, mainly the methyl mercury species found in HLW samples, that could form VOCs such as methane or ethane. If radiolysis or thermolysis leads to C-Hg bond breakage in methyl mercury, then subsequent reactions are postulated that could account for methane, methanol, hydrogen and ethane production via Equations 1-5 below. Equations 2-5 are taken from gas phase chemistry of the methyl radical but can also be postulated to take place in caustic aqueous tank waste containing soluble organics identified as 'RH'. Equation 6 represents a hydrolysis reaction that could form methane, mercury(II) oxide and a protonated form of the counter anion in the original methyl mercury species such as the indicated nitrate anion. Other reactions of hydrated methyl mercury in caustic solution have been proposed that incorporate the methyl mercury into dimers and trimers with no production of methane.[53,54] These reactions are shown in Equations 7-9.
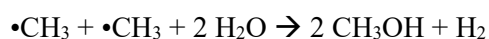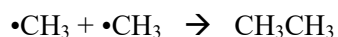
$$CH_3\text{-}Hg^+X^- -Heat \rightarrow \bullet CH_3 + Hg^+X^- \qquad \text{Equation 1}$$

$$\bullet CH_3 + RH \rightarrow CH_4 + R\bullet \qquad \text{Equation 2}$$

$$\bullet CH_3 + R\bullet \rightarrow RCH_3 \qquad \text{Equation 3}$$

$$\bullet CH_3 + \bullet CH_3 + 2\ H_2O \rightarrow 2\ CH_3OH + H_2 \qquad \text{Equation 4}$$

$$\bullet CH_3 + \bullet CH_3 \rightarrow CH_3CH_3 \qquad \text{Equation 5}$$

$$CH_3\text{-}Hg^+NO_3^- + H_2O \rightarrow CH_4 + HgO + H^+NO_3^- \qquad \text{Equation 6}$$

$$CH_3\text{-}Hg(OH_2)^+ + OH^- \rightarrow CH_3\text{-}HgOH + H_2O \qquad \text{Equation 7}$$

$$CH_3\text{-}Hg(OH_2)^+ + CH_3\text{-}HgOH \rightarrow (CH_3\text{-}Hg)_2OH^+ + H_2O \qquad \text{Equation 8}$$

$$CH_3\text{-}HgOH + (CH_3\text{-}Hg)_2OH^+ \rightarrow (CH_3\text{-}Hg)_3O^+ + H_2O \qquad \text{Equation 9}$$
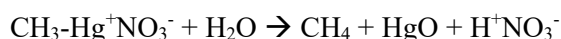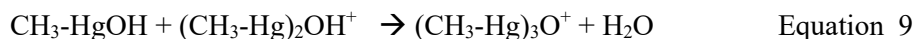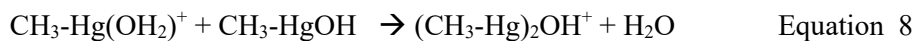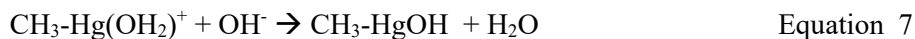
Investigations on thermolysis of low concentration dimethyl mercury (402 ng in 0.250L = 1.61E+03 ng/L or 1.61E-3 mg/L (6.97E-09 M)) under various pH conditions and temperatures was performed by the Frontier Geosciences Aquatic Research Group for SRS in 2003 resulting in the data shown in Table 2-14 and Table 2-15.[55] The 7 M NaOH system shown in the grey-scale highlighted rows is representative of tank waste simulant, the pH 10 NaOH system is representative of condensate simulant and the acidic systems are representative of simulated acidified wastes to Waste Water Treatment Plant (WWTP).[55] These data from Table 2-14 indicate that dimethyl mercury decomposes in caustic waste simulant indicated in the rows with grey shading with a half-life of 154 hours at the highest temperature studied (83°C). These tests did not measure volatile gases such as hydrogen or VOCs produced in the decomposition. Table 2-15 shows that most of the original ~ 1.6 ng/mL dimethyl mercury decomposed to methyl mercury in the acidic pH = 2.0 solutions when held for 91 h at the temperatures shown. Presence of methyl mercury in these samples also suggests that the methyl mercury decomposition product was relatively stable compared to the starting dimethyl mercury. The dimethyl mercury was relatively stable in the pH = 10 solutions for short times (91 h) at high temperature of 83°C or long times (547 h) at low temperature of 39°C. The last two rows of Table 2-15 involving pH = 10 or 7M NaOH at long times of 547 h and maximum temperature of 83°C suggest that the original dimethyl mercury is more stable in the pH 10 solution (0.73 ng/mL remaining) than the 7 M NaOH solution (0.13 ng/mL remaining). Neither of these systems appeared to produce methyl mercury in the acidic systems. An explanation suggested is that in these caustic cases, the dimethyl mercury is more fully degraded, either to Hg(II) or Hg°, suggesting that any methyl mercury produced also decomposed during the 547 h exposure.[55]

Table 2-14. Decomposition Half-lives for Dimethyl Mercury in Various Matrices[55]

Matrix	Calculated decay half-life (hours)		
	39 ºC	65 ºC	83 ºC
7M NaOH + 1M NaNO$_3$ + 1M NaNO$_2$	814	276	154
pH 10 (NaOH + NaNO$_3$ + NaNO$_2$)	9,565	1,929	617
pH 2.0 (HCl + glycine)	16.4	5.6	2.7
pH 2.0 (HNO$_3$)	11.8	3.1	0.9

Table 2-15. Observed Methyl and Dimethyl Mercury Remaining in Degradation Samples[55]

Sample ID	Mercury Concentrations, ng/mL		
	CH$_3$Hg$^+$	(CH$_3$)$_2$Hg	Sum
83°C, pH 2.0 HCl, 91 h	1.25	0.00	1.25
65°C, pH 2.0 HCl, 91 h	1.42	0.00	1.42
39°C, pH 2.0 HCl, 91 h	1.45	0.04	1.49
83°C, pH 10.0, 91 h	0.02	1.40	1.42
39°C, pH 10.0, 547 h	0.00	1.41	1.41
83°C, pH 10.0, 547 h	0.01	0.73	0.74
83°C, 7M NaOH, 547 h	0.01	0.13	0.14

Data shown in Table 2-14 can be used to determine an activation energy for dimethyl mercury in the 7 M NaOH system. Figure 2-14 shows the half-life values plotted vs. the temperature in Celsius. The first three half-lives are from Table 2-14 and the additional four higher temperatures are calculated from the best fit exponential function derived from the initial three data pairs. Table 2-16 shows the temperature and half-life data (experimental derived and extrapolated) for Figure 2-14. As indicated by Bloom a plot of the natural log of the experimental rate constant (ln(k)) vs. reciprocal absolute temperature (1/T) should yield a straight line equal to the activation energy for dimethyl mercury decomposition divided by the ideal gas constant, or slope = $-E_a/R$. Using data from Table 2-16, Figure 2-15 shows the plot of ln(k) vs. 1/T with slope = -4,225. Multiplying this value by R = 8.31E-03 kJ/mol/K, gives an activation energy of ~ 35 kJ/mol for the 7 M NaOH solution.

The data discussed above from Bloom can be used to estimate a methane generation rate from the thermal decomposition of dimethyl mercury at the potential maximum concentration in SRS tank waste of ~ 1 mg/L. In this example, the dimethyl mercury decomposition rate is assumed to be first order and produces 1 mole of methane (via the methyl radical) for every mole of dimethyl mercury decomposed via Equation 10.

$(CH_3)_2$-Hg –(thermolysis)$\rightarrow$ CH_3-Hg^+X^- + •CH_3 (conversion of •CH_3 to CH_4)   Equation 10
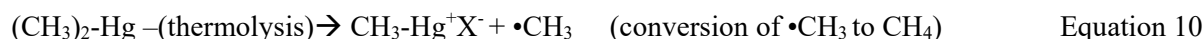
Table 2-17 shows the experimentally determined dimethyl mercury half-lives and the extrapolated half-lives at the various temperatures and the corresponding methane generation rates given the above assumptions. The final column of Table 2-17 shows the methane generation rates in the units of ft^3/gal/h calculated at the specific temperatures, which range from 9E-09 ft^3/gal/h at 39°C up to 1.9E-06 ft^3/gal/h at 170 °C. This contribution would be short lived given the low sub-mg/L analyzed concentrations of dimethyl mercury in waste samples.[42,44]
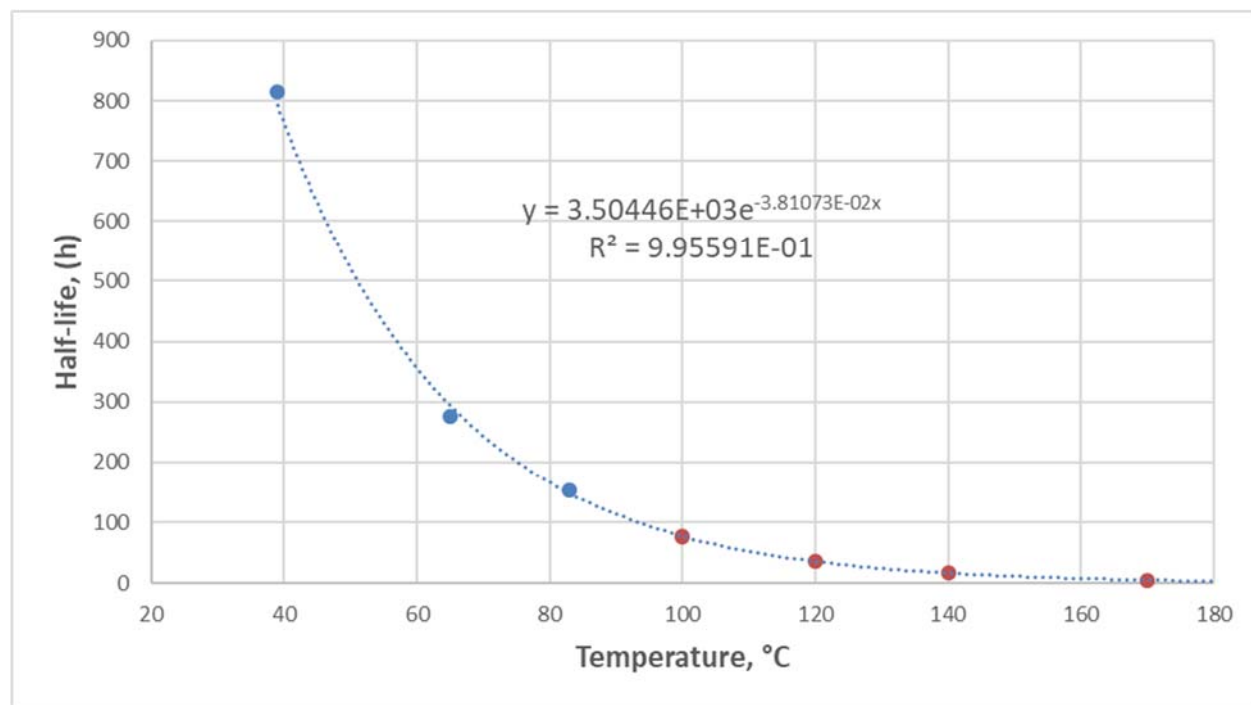

Figure 2-14. Half-life for Dimethyl Mercury vs. Temperature (°C)

(NOTE: extra digits retained for equation although all are not statistically significant.)

Table 2-16. Experimental and Calculated Half-lives and Experimental Rate Constants for Dimethyl Mercury Decomposition in 7M NaOH Simulated Tank Waste

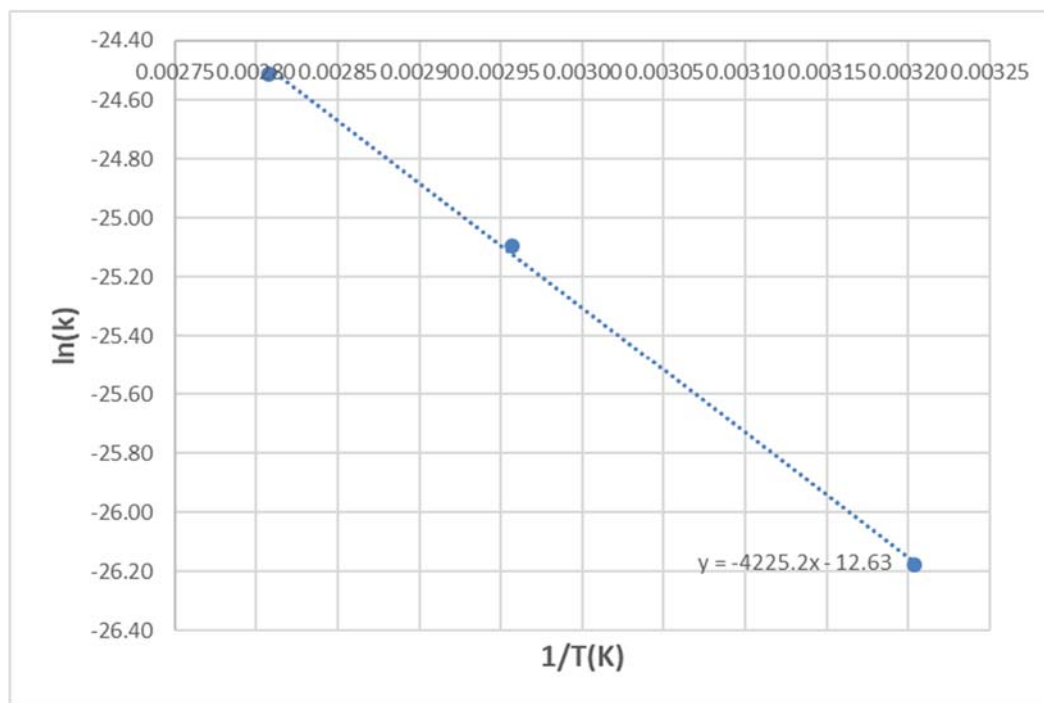| T (°K)	7M NaOH, 1M NaNO₂, 1M NaNO₃ T (°C)	Measured Half-life (h)	Calculated Half-life (h)	Initial Concentration (M)	k (M/h)	ln(k)	1/T(°K)
312.15	39	814	792.8	6.97E-09	4.28E-12	-26.18	0.00320
338.15	65	276	294.4	6.97E-09	1.26E-11	-25.10	0.00296
356.15	83	154	148.2	6.97E-09	2.26E-11	-24.51	0.00281
373.15	100	NA*	77.6	NA	NA	NA	NA
393.15	120	NA	36.2	NA	NA	NA	NA
413.15	140	NA	16.9	NA	NA	NA	NA
443.15	170	NA	5.4	NA	NA	NA	NA

*NA = not applicable

Figure 2-15. Plot of ln(k) vs. 1/T(K) for Dimethyl Mercury Decomposition in 7M NaOH Simulated Tank Waste

(NOTE: extra digits retained for equation although all are not statistically significant.)

Table 2-17. Calculated Methane Generation Rates from Dimethyl Mercury Decomposition in 7M NaOH Simulated Tank Waste

T (°C)	T(K)	Half-life (h)	mol/(L-h)	mol/(gal-h)	at 298.15 K ft³/(gal-h)	at Temp. K ft³/(gal-h)
39	312.15	814	2.66E-09	1.01E-08	8.71E-09	9.12E-09
65	338.15	276	7.85E-09	2.97E-08	2.57E-08	2.91E-08
83	356.15	154	1.41E-08	5.33E-08	4.60E-08	5.50E-08
100	373.15	77.6	2.79E-08	1.06E-07	9.14E-08	1.14E-07
120	393.15	36.2	5.99E-08	2.27E-07	1.96E-07	2.58E-07
140	413.15	16.9	1.28E-07	4.86E-07	4.20E-07	5.82E-07
170	443.15	5.4	4.03E-07	1.52E-06	1.32E-06	1.96E-06

The decomposition of low ng/L levels of methyl mercury has been investigated in reagent water and filtered lake sediment pore water in the temperature range of 5 °C to 26 °C.[56] These tests also considered the effect of incandescent light exposure. Table 2-18 shows the decomposition rates for the reagent water samples as a function of light exposure and temperature, and Table 2-19 shows data for the filtered pore water samples conducted in the dark at 26 °C. No information was given as to the specific pH of these systems, but it is assumed that both the reagent water and filtered pore water are neutral with pH ~ 7. Decomposition rates were calculated from plotting $\ln((\text{methyl mercury})_t/(\text{methyl mercury})_{t=0})$ vs. time. This data was used to calculate the 20-day methyl mercury decomposition rate from the reagent water system reacted in the absence of light at 50 ng/L. Using this rate of 4.1E-13 mol/L/day with a starting concentration of methyl mercury at 200 mg/L near the analyzed maximum in SRS tank waste, one calculates a decomposition rate of 1.64E-6 mol/L/day. Evaluation of the reagent water data sets at the two temperatures of 5 °C and 26 °C gives an average activation energy of 90.3 kJ/mol ± 22.1 kJ/mol. Using the highest methyl mercury decomposition rate of 1.64E-6 mol/L/day and the average activation energy of 90.3 kJ/mol from the reagent water data set, one can calculate a methyl mercury decomposition rate at higher temperatures via the Arrhenius Equation 11 below.

$$\log (k_1/k_2) = (E_a/2.3*R) * (1/T_2 - 1/T_1) \qquad \text{Equation 11}$$
where,
k = rate constant (units of day^{-1} for decomposition of methyl mercury; units of mol/L/day for production of methane)
E_a = activation energy = 113 kJ/mol for H_2 from glycolate thermolysis
R = 8.314 J/K-mol, the gas constant
T = the waste temperature in Kelvin

If one conservatively assumes that one mole of methane could potentially be produced from decomposition of methyl mercury via fast methyl radical conversion/reaction to methane (i.e., Equations 1 and 2 along with the hydrolysis reaction shown in Equation 6 occur, while Equations 3-5 and 7-9 are dismissed), then the methane production rates can be estimated from the methyl mercury decomposition data in pure water. Table 2-20 shows results of estimated methane generation rates up to 170 °C. These estimated methane generation rates from methyl mercury in neutral water in the range of 2.2E-07 ft³/gal/h at 26 °C up to 4.5E--02 ft³/gal/h at 170 °C are higher than the methane generation rates for each specified temperature estimated from the dimethyl mercury decomposition data from 7 M NaOH simulated tank waste shown in Table 2-17.

Table 2-18. Methyl Mercury Decomposition Rate Constants in Reagent Grade Water[56]

Treatment		k_d (d^{-1})
1 ng/L	Dark, 5 °C	0.0009 ± 0.0013
	Dark, 26 °C	0.0363 ± 0.0263
	Light, 5 °C	0.0063 ± 0.0029
	Light, 26 °C	0.0541 ± 0.0324
5ng/L	Dark, 5 °C	0.0023 ± 0.0010
	Dark, 26 °C	0.0272 ± 0.0165
	Light, 5 °C	0.0087 ± 0.0031
	Light, 26 °C	0.1225 ± 0.0150
50 ng/L	Dark, 5 °C	0.0019 ± 0.0015
	Dark, 26 °C	0.0018 ± 0.0015
	Light, 5 °C	0.0037 ± 0.0021
	Light, 26 °C	0.0055 ± 0.0023

Table 2-19. Methyl Mercury Decomposition Rate Constants in Filtered Lake Sediment Pore Water[56]

Treatment	k_d (d^{-1})
1 ng/L	0.0178 ± 0.005
5 ng/L	0.0154 ± 0.005
50 ng/L	0.0212 ± 0.005
–Control	0.0044 ± 0.002

Table 2-20. Calculated Methane Generation Rates from Methyl Mercury Decomposition in Water

T (°C)	T(K)	mol/L/day	mol/L/h	mol/(gal-h)	at 298.15 K ft^3/(gal-h)	at Temp. K ft^3/(gal-h)
26	299.15	1.64E-06	6.83E-08	2.59E-07	2.23E-07	2.24E-07
50	323.15	2.44E-05	1.02E-06	3.85E-06	3.33E-06	3.60E-06
75	348.15	2.74E-04	1.14E-05	4.32E-05	3.73E-05	4.35E-05
100	373.15	2.22E-03	9.25E-05	3.50E-04	3.02E-04	3.78E-04
120	393.15	9.78E-03	4.07E-04	1.54E-03	1.33E-03	1.76E-03
140	413.15	3.73E-02	1.55E-03	5.88E-03	5.08E-03	7.04E-03
170	443.15	2.22E-01	9.24E-03	3.50E-02	3.02E-02	4.49E-02

2.6 Thermolysis Reactions in Caustic Solution Related to the Bayer Industrial Process

Thermolysis degradation of organic compounds present in Bayer Process liquors has been studied recently by Costine and co-workers.[9,10,11,12] This process is an analog of the aluminum leaching process at SRS although the temperatures are appreciably higher. Some of these references were noted in the recent study related to hydrogen production from radiolytic and thermolytic degradation of either formate or glycolate in SRS Tank Farm wastes.[57]

Table 2-21 shows a summary of the various organic compounds studied for thermolysis in caustic solutions in the Costine series of papers. Table 2-22 summarizes details of the four investigations with a focus on the main findings concerning the ratio of the product hydrogen to parent organic starting compound in the final column. The complete list of chemicals studied in each series is given in Appendix A. These tests used sealed systems performed in an autoclave with subsequent gas and solution analysis performed on cooled, sealed samples. Hydrogen concentrations in the headspace were measured using online electrochemical sensors fit with gas permeable membranes which regulated gas flow to the sensor and limited hydrocarbon gas flow to the sensor. The detection limit for hydrogen analysis was indicated as 0.01 mol%. The first two papers in this series[9,10] focused exclusively on hydrogen as the measured gaseous products and did not address the potential formation of hydrocarbon gases. The latter two papers in the series[11,12] did address possible formation of hydrocarbon gases. Although volatile organic carbon gaseous species were not analyzed in the head-space gas for these studies,[11,12] detailed pre/post reaction solution characterization was performed to investigate the aqueous carbon balance. For instance, in the degradation of polyols study[11] the authors state,

> "Carbon recoveries, defined as the ratio of the number of moles of organic and inorganic carbon in the solution products to the initial number of moles of carbon in the starting polyols (expressed as a percentage), were determined by a Shimadzu TOC-V CPH/CPN total organic carbon (TOC) analyzer. For all polyols studied, recoveries of carbon in the aqueous phase were between 97 and 106%, indicating that the formation of gaseous hydrocarbons was insignificant."

In the wet oxidation of industrial bayer liquor study,[12] the authors state,

> "Direct evidence for the progressive formation of smaller molecules from High Molecular Weight (HMW) substances is presented in Figure 1B, with oxalate and carbonate appearing as dominant, stable products with increasing TOC conversion. The ultimate degradation product of organic compounds is carbon dioxide (present in alkaline solutions as carbonate), and is therefore continuously formed in the Bayer liquor circuit. The extent of TOC conversion after 3 h at 270 °C was 43%, which was almost fully converted (99%) to carbonate in the liquor. This result indicates that the loss of carbon from the liquor through the formation of hydrocarbon gases such as methane was negligible."

Several instrumental techniques including capillary electrophoresis and ion chromatography were used to measure the concentrations of various organic species, and the concentration of carbonate in the solutions was measured using an automated potentiometric titration system. Carbon recoveries determined from Total Inorganic Carbon (TIC) and TOC also used a total organic carbon analyzer.

The main conclusions from these studies include the variable hydrogen to parent organic molar ratios shown in Table 2-22. Another relevant finding based on the detailed carbon balances performed is that insignificant or negligible amounts of gaseous hydrocarbons were formed in this testing. However, this conclusion is exclusively based on solution phase carbon analyses and would appear to need supporting evidence via actual head-space gas analysis for non-condensable hydrocarbon gaseous species. The initial study[9] also cited analysis of digestion vent gases of a Queensland alumina refinery in Australia that showed emissions consisting of 2% non-condensable gases in steam formed in the ratios of 98.7% hydrogen, 8.6% nitrogen, 1.2% of methane and other hydrocarbons, carbon oxides at 0.3% and oxygen at 0.2%. Thus, the molar ratio of methane to hydrogen was < (1.2%/98.7%), or < 0.013.

The thermolysis reactions were also studied as a function of temperature at fixed hydroxide concentration, and as a function of increasing hydroxide concentration at fixed temperature. Activation energies for hydrogen formation were reported in the range of 140-144 kJ/mol and 158-176 kJ/mol in the temperature ranges of 200-250 °C and 200-275 °C, respectively. Hydroxide concentrations were found to have a significant influence on the production of hydrogen over the range of 0-6 M. These results suggest a base-

catalyzed reaction involving deprotonation of the parent organic as the rate limiting step via Equations 12 and 13:

$$RH + OH^- \rightarrow R^- + H_2O \qquad \text{Equation 12}$$
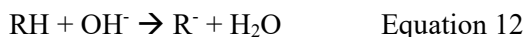
$$R^- \rightarrow products \qquad \text{Equation 13}$$

Table 2-22 indicates that the molar ratio of product hydrogen to starting parent organic depends strongly on the starting organic structure with values ranging from <0.25 to 2. Hence, it is useful to contrast the predominant compounds and structures in SRS tank waste[38] with those explored by Costine et al. For instance, the ion exchange resins at SRS fall within the grouping akin to carboxylates, while the solvents are aliphatic hydrocarbons. The antifoams with siloxane backbone and multiple hydroxyl groups are in some ways analogs of the polyol category.

Expectations then are that solvent compounds will tend to produce limited amounts of hydrogen while undigested resin transferred to the SRS Tank Farm risk producing more moderate amounts of hydrogen. The inference for antifoam agents is more speculative. They contain the multiple hydroxyl groups that appear vulnerable to chemical attack via thermolysis as

- *Methane and other hydrocarbon formation in the Bayer process from thermolysis tends to show a hydrogen-to-methane molar ratio of ≥75 (albeit at temperatures more extreme the SRS waste processing conditions).*
- *Studies of the Bayer process (from 2011 to 2016), albeit at more extreme conditions (175 °C to 275 °C), with a wide range of compounds provide insight into the relative stability of classes of compounds toward hydrogen formation. By extrapolation and comparison to organics in SRS waste, antifoam is expected to show higher propensity for hydrogen (or flammable gas) formation. Ion exchange resins and solvents, in decreasing order, will likely yield lower quantities per unit mass of starting organic.*

well as methyl moieties that may be an ultimate source of free methane. These compounds may pose greatest risk of contributing to increased methane or flammable VOC production.

Recall that the relative amounts of these species transferred to SRS waste historically[5,6] is thought to decrease in the order: solvent, digested ion exchange resins, undigested ion exchange resins, and antifoams. Most transfers ceased with curtailment of PUREX separation operations in the Canyon facilities and suspension of antifoam use in the CSTF evaporators. Projection of a methane-to-hydrogen ratio from analogy to the work of Costine et al. is not possible. Nevertheless, a balanced interpretation of the relative amounts of source organics, the kinetics of the degradation reactions, the high volatility of the produced flammable compounds, and the elapsed time favor a lower ratio of methane-to-hydrogen within the demonstrated range for these compounds.

Table 2-21. Summary of Various Organic Compounds Used in Caustic Thermolysis Tests

Ref. [9]	Aliphatic and Aromatic Hydroxycarboxylic Acids (Table A-1 in Appendix A for detailed listing)
Ref. [10]	Unsaturated Hydroxycarboxylic Acids (Table A-2 in Appendix A for detailed listing)
Ref. [11]	Aliphatic polyols (alditols) and five carboxylates (glycolate, pyruvate, glycerate, lactate and acrylate) (Table A-3 in Appendix A for detailed listing of the polyols)
Ref. [12]	Aliphatic compounds (3-hydroxybutanoic acid, maleic acid, and erythritol) Aromatic compounds (benzoic acid, m-salicylic acid, gallic acid, and catechol), Acetaldehyde, butyraldehyde, benzaldehyde, and glyoxylate

Table 2-22. Summary of Results from Various Caustic Thermolysis Tests

	Temp. °C	Hydroxide Concentration	Atmosphere	Reaction Times (h)	Gases Detected*	Moles(H_2): Moles(Parent C)
Ref. [9]	175 - 275	3.77M; (0 - 6M) study effect of OH-	anaerobic	> 120	H_2	<0.25 for aliphatic & aromatic carboxylate & aromatic hyrdoxycarboxylate & phenol; 0.25-1 for aliphatic hydrocarbon
Ref. [10]	175 - 275	3.77M; (0 - 6M) study effect of OH-	anaerobic	> 120	H_2	~ 1 for unsaturated carboxylates
Ref. [11]	250 - 275	3.77M	anaerobic	> 300	H_2**	~ 2 for polyols
Ref. [12]	180 - 270	3M	N_2 or wet ox(O_2)	> 180	H_2***	NA****

*Only gaseous species analyzed was hydrogen.
**Recovery of carbon in liquid products by TOC measurement in range of 97-106%, suggesting formation of gaseous hydrocarbons 'insignificant'.
***Extent of TOC conversion after 3 h at 270C was 43%, which was almost fully converted (99%) to carbonate in the liquor indicating loss of carbon from the liquor through formation of hydrocarbon gases such as methane was negligible.
****No Moles(H_2):Moles(Parent C) ratios reported[12] for this testing of Aliphatic and Aromatic compounds listed in final row of Table 2-21.

2.7 Thermolysis Studies Performed for Caustic-Side Solvent Extraction

Numerous studies examined the thermal and radiolytic stability of solvent systems used at SRS for cesium separation.[58,59,60,61,62,63,64,65] These reports typically involve temperatures for thermolysis from 35 °C to 61 °C. The 35 °C temperature is the maximum sustained temperature assumed for the stripping section of the CSSX system. The primary focus of a number of these studies involves investigation of processing parameters of the solvent system (extraction, scrubbing, stripping, etc.) and how they are sustained with respect to thermolysis. A subset of the reports focused chiefly on thermolysis and gas product analysis.[63,64,65] Sections 3, 4 and 9 of the Flammable Gas Generation Mechanisms report addressed details

of radiolytic and thermolytic decomposition for some of the various components that comprise both the original and the next generation solvent extraction systems (Table 3.4.1: BOBCalixC6 CSSX and NG-CSSX solvent components).[3] The diluent Isopar® L, which is a C-12 isoparaffinic flammable hydrocarbon, is the highest mass fraction component and is identified as potentially present in DWPF at the limit of 87 mg/kg per the Flammable Gas Generation Mechanisms report[3] and in Tank 50 with a current WAC limit of 11 ppm.[19] The current Tank 50 WAC revision applies to Low Isopar L Operation[19] and this value may increase to the 87 mg/kg value for future processing in the Salt Waste Processing Facility.[3]

Chemical stability ("thermolysis") testing with the original CSSX system performed at Oak Ridge National Laboratory (ORNL) showed that processing parameters were sustained up to 235 days at temperature of 35 °C. The solvent component noted for greatest chemical instability is the minor suppressor component tri-n-octylamine that degraded to dioctylamine in a 110-day study at 61 °C.[58] Williams et al. from ORNL performed thermal and radiolytic degradation work in 2011 on the Next Generation CSSX (NG-CSSX) solvent system at temperatures up to 35 °C in various matrices including a caustic SRS simulant, 25 mM NaOH and 10 mM H_3BO_3.[62] This unpublished letter report showed that degradation was more evident in caustic solutions than in boric acid. These tests[62] focused on cesium distribution ratios and their behavior as a function of accumulated dose and temperature through a 5-month period. Data contained in the Williams et al. letter report[62], as well as other unpublished reports pertaining to NGS has been qualified by SRR personnel.[66]

> *Combined thermolysis and radiolysis studies for the cesium removal (CSSX) solvent suggest a potential methane-to-hydrogen ratio near ~0.24 with lesser amounts of other VOCs. This magnitude agrees reasonably well with radiolysis data for PUREX solvent.*

Moyer et al. identified several decomposition products (designated as 'DCU', 'iTDA', and 'TCHG' in Table 2-23) derived from either thermolysis (maximum temperature of 35°C) or radiolysis of the NG-CSSX in studies performed at ORNL.**[61]** The NG-CSSX uses the guanidine based suppressor and some of the degradation products are actually similar to 'impurities' in the waste from ion exchange resin (Table 2.1 of Moyer et al.[61]). A modifier decomposition product is also present as an impurity shown as 'SBP'. Roach et al. further detailed the degradation products from thermal treatment of the NG-CSSX[59] by use of electrospray mass spectroscopy to identify the 'Isotridecylamine' (iTDA) shown in Table 2-23. The authors state,

> "The mass spectra qualitatively show the production of isotridecyl amine, a product of guanidine hydrolysis, implying that the guanidine degradation mechanism is the simple and chemically reasonable attack of hydroxide on the guanidine".

This reaction can be generally represented as,

Suppressor (DCiTG LIX79) – (hydrolysis, hydroxide, heat) → DCiTGnidine(DCU) + DCiTGnidine(iTDA)

where DCU is N,N'-Dicyclohexylurea and iTDA is isothridecylamine.

Of all the decomposition products discussed above for the CSSX system, only 'iTDA' and 'SBP' contain methyl groups that could be postulated as source for methyl radical production on subsequent thermolytic or radiolytic decomposition of the NG-CSSX system.

The most insightful study for formation of flammable VOCs for the original CSSX solvent formulation covered the range of 17 to 43 °C.[64] Those experiments subjected CSSX solvent to 32.2 Mrad irradiation dose with subsequent analysis of the vapor space. The study provides estimates for relative amounts of methane and hydrogen produced (as well as values for 12 other organic species). A number (7) of the compound identifications are tentative as the testing did not include calibration for those species. The methane-to-hydrogen molar ratio measured ~0.24 and the (C_2 through C_6 hydrocarbon)-to-hydrogen molar ratio is lower at ~0.06. Table 2-24 provides summary information and the reader is referred to the source document for more complete listing. Although these studies lack independent verification, the production rates determined have similar magnitude to those for studies of the PUREX solvent system in the 'Radiolytic Behavior' chapter of Reference 67.

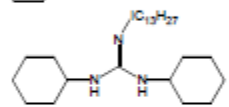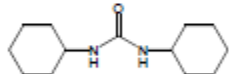**Table 2-23. NG-CSSX Solvent Components and Possible Degradation Products from ORNL Testing[61]**

Table 11.1. NG-CSSX solvent components and possible degradation products
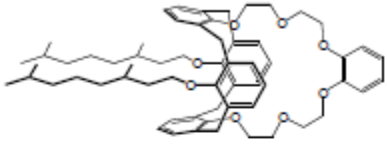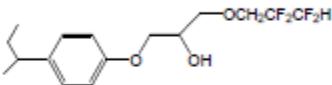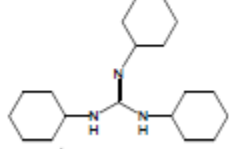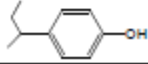
Component	Code	Chemical Name	Structure
Extractant	MaxCalix	1,3- *alt*-25,27-Bis(3,7-dimethyloctyl-1-oxy) calix[4]arene-benzocrown-6	
Modifier	Cs-7SB	1-(2,2,3,3-Tetrafluoropropoxy)-3-(4-*sec*-butylphenoxy)-2-propanol	
Suppressor	DCiTG or LIX 79	*N,N*-Dicyclohexyl-*N''*-isotridecylguanidine	
Diluent	Isopar L	C_{12}-isoparaffinic hydrocarbon	
DCiTGnidine Impurity 1	DCU	*N,N*-Dicyclohexylurea	
DCiTGnidine Impurity 2	iTDA	Isotridecylamine	$iC_{13}H_{27}NH_2$ (branched alkyl chain averaging approx. 10 carbons long)
DCiTGnidine Impurity 3	TCHG	*N,N,N''*-Tricyclohexylguanidine	
Modifier Impurity	SBP	4-*sec*-Butylphenol	

Table 2-24. VOCs from Extended Dose Irradiation of CSSX Solvent[63]

Compounds	Relative Molar Amounts
Hydrogen	1.08
Methane	0.26
C_2 to C_6 alkane hydrocarbons	0.069
Other tentatively identified VOCs	0.051

2.8 Antifoam Degradation Studies

Antifoam 747 is used in the DWPF and many reports discuss the antifoam degradation products (ADPs) from hydrolysis degradation in radiolytic and thermolysis processes encountered in the DWPF chemical process cells.[68,69,70,71,72,73,74,75] The Flammable Gas Generation Mechanisms review[3] cited these references in sections 3, 4 and 9 with the main emphasis relating to hexamethyldisiloxane (HMDSO), trimethylsilanol (TMS), and propanal. Each of these is a National Fire Protection Association (NFPA) Class 2 flammable liquid defined as combustible liquids that have a flash point at or above 100 °F and below 140 °F. References from 2013 to 2015 mainly relate to the formation and analysis of the ADPs, whereas references from 2016 address the ADP formation rates and their chemical properties and kinetic behavior. The 2015 study examined two samples collected from different elevations of Tank 22 and found that TMS was the only detectable species at 2.7 mg/L.[72] The February 2016 study analyzed actual DWPF processing samples to show both HMDSO and propanal near or below the detection limits (0.25 mg/L for both) for the analysis and the TMS present up to 11 mg/L.[71] Low amounts of total organic carbon in the range of 3 to 39 mg/L were attributed to the presence of formate which was also measured by ion chromatography. Although volatile organic analysis (VOA) and semi-volatile organic analysis (SVOA) were used in this work, emphasis was placed on detection of the three ADPs and no information was given regarding any other volatile or semi-volatile compounds that may have been present.

Prior testing on offgas production from thermolysis or radiolysis of antifoam does not provide insight into whether lighter VOCs formed.

Current laboratory testing with caustic simulants seeks to investigate the hydrogen formation potential of the ADPs under thermolysis conditions, with the exclusion of HMDSO due to its relative low water solubility.[38] Methane production from these tests is also measured. To SRNL's knowledge there has not been laboratory study of potential thermolysis effects on the individual ADPs in caustic solutions with respect to VOC formation including temperatures up to and including SRS Tank Farm evaporator temperatures. Table 2-25 taken from the 2016 SRNL study[73] shows that the structure of each of the ADPs contains end unit methyl group(s). As was pointed out in Hanford-related studies involving radiation and thermolysis and the synergistic effects of both processes in caustic waste and simulants, production of methane, methanol and other low-carbon containing VOCs can be attributed to methyl radical reactivity (see Table 2-13 and Equations 2-5 above). Thus, it is conceivable that these ADPs could produce VOCs (involving a methyl radical formed from degradation of a parent ADP) in addition to their potential role in hydrogen production from thermolysis. One example of this behavior is the preliminary finding from SRNL testing[38] that methane is produced at ~ 10X the rate as hydrogen from thermolysis testing of TMS in a Tank 38 simulant. Methylated silane compounds contain methyl groups and thus are a feasible source of methane upon decomposition. In addition, aldehydes (formaldehyde, and by extension propanal) have been shown by Ashby[35] to contribute to thermolytic hydrogen generation.

Table 2-25. ADP Structures from a Previous SRNL Study[73]

Table 2-2. Antifoam Degradation Products

Compound	Formula	Structure	Molar Mass, g/mol	Solubility in water	Lower Flammability Limit, vol %	Boiling Point
Hexamethyl disiloxane (HMDSO)	$C_6H_{18}OSi_2$	CH₃ CH₃ H₃C—Si—O—Si—CH₃ CH₃ CH₃	162.38	0.933 mg/L @ 23 °C	0.8	100 °C
Trimethyl silanol (TMS)	$C_3H_{10}OSi$	OH H₃C—Si—CH₃ CH₃	90.20	35 g/L @ 25 °C	1.45	99 °C
Propanal	C_3H_6O	H H O H—C—C—C H H H	58.08	310 g/L @ 25 °C	2.6 -2.9	46-50 °C

2.9 Tri-butyl Phosphate Degradation

The PUREX solvent system consisting of kerosene with nominally ~ 30 wt % tri-butyl phosphate (TBP), is addressed in the Flammable Gas Generation Mechanism report in Sections 3 and 4.[3] It is generally acknowledged that the kerosene diluent evaporates quickly and is not present in significant amounts within SRS waste as verified by measurements in pump tanks that receive discards, waste in storage tanks and vapor samples (Section 3.4).[3] The TPB decomposes in caustic solution through hydrolysis to produce dibutyl phosphate (DBP) and butanol, with subsequent slower conversion of DBP to monobutyl phosphate and butanol. Gaseous products from radiolysis of neat TBP include hydrogen and a variety of C_1-C_7 VOCs.[67] Several studies related to the degradation of TBP were cited that involved analysis of radioactive tank samples[76,77] and caustic simulants.[78]

Analysis of five different SRS CSTF samples (from Tanks 23, 30, 33, 43 and 46) in 2003 by the Pacific Northwest National Laboratory PNNL) showed a maximum TOC concentration of 200 mg/L for these particular five tanks.[76] These tanks were chosen as representative of five waste tanks expected to pose the highest potential to contain radiolytic and chemical decomposition products from added organics.[3] Headspace analysis of these samples only showed a single sample from Tank 33 that contained ~ 7 mg/L butanol, with no detection of trimethylamine, 4-ethylbenzyl alcohol, benzene, and toluene. No TBP was found in the samples at a detection limit of 5 mg/L and the maximum DBP and MBP were 78 mg/L and 43 mg/L, respectively.

Analysis of seven different SRS Tank Farm samples (from Tanks 13, 30, 37, 39, 45, 46 and 49) obtained in the timeframe of May through October of 2003 indicated TOC in the range of 960 to 2,730 mg/L with only three of the tanks showing detectable VOC concentrations in the range of 9.7 to 28.1 mg/L and no detectable SVOA analytes.[77] No speciation or identification of specific species were given in the three tanks that showed detectable VOC. These analyses also showed no TBP at detection limits of 1 to 50 mg/L and only a single Tank 13 had detectable DPB at 1,610 mg/L with all other tanks having DBP values at nominally < 500 mg/L. No information was given in the technical report to indicate the temperatures of the tanks at the time of sampling.[77]

The simulant study investigated TBP hydrolysis as a function of temperature in the range of 40°C to 110 °C.[78] Rates for the TBP hydrolysis were also described by Britt[7] with reference to other studies that

confirm the instability of TBP in caustic solution. The simulant study also included text describing results from actual waste and pump tank samples.[78] Conclusions from those analyses stated,

> *"Analysis of samples from a number of waste and pump tanks indicated the concentration of organic species to be extremely low in all samples. The worst case was Pump Tank 3F where 230 mg/L TBP and 77 mg/L n-paraffin were found; the concentrations of the remaining organics in the tanks were in the low mg/L range. No organic species were found in most vapor samples, and only nanogram/L quantities of organics were found in a few of the vapor samples."*

Current thermolysis testing will use dibutyl phosphate and butanol as the main TBP decomposition products to access hydrogen generation rates.[38] As is the case with the ADPs, these TBP degradation products also contain methyl groups that could be postulated as the source of methyl radical chemistry leading to thermolysis VOCs production. However, the TBP degradation products also contain C-OH and C-O bonds in their structure which could provide lower energy decomposition pathways not leading to methyl radical formation.

> *Decomposition of tributyl phosphates and the degradation products in alkaline media is well studied. The authors found no literature evidence of methane generation from this reaction system.*

2.10 Spent Ion Exchange Resins

Degradation of spent ion exchange resins was examined in Section 3 and 4 of the Flammable Gas Generation Mechanism report.[3] That review[3] noted that, according to Walker's assessment of organic compounds in SRS HLW,[5] the majority of original resin material was digested in alkaline permanganate before discharge to the SRS Tank Farms, although some direct discharges occurred.[79] Some resin degradation products mentioned in the radiolysis section indicate production of carbon dioxide, hydrogen, trimethylamine and methane. Tank sampling shows evidence of trace concentrations of the fragment compounds (alcoholic $R-C_6H_4-CH_2-OH$ and carboxylic $R-C_6H_4-COOH$ and aliphatic tertiary amines such as trimethyl amine $N(CH_3)_3$).[5,76] The 'R' grouping in the above compounds could be $-N(CH_3)_3^+$ or $-C_5H_4N(CH_3)^+$ for anion resins and $-C_6H_5SO_3^-$ for cation resins.[5] It was concluded in Section 3 of the Flammable Gas Generation Mechanism report[3] that low contributions to flammable gas burden exist for radiolytic degradation of the spent resins. Section 4 'Thermolysis Releasing Other Flammable Compounds' provides general discussion of the digested resins and degradation products expected from radiolysis of polystyrene or styrene-divinylbenzene copolymer resins with references given to the Walker[5] and Hobbs[6] reviews. No specific thermolysis studies investigating the degradation products expected from spent resins or resin fragments in caustic solution were cited.

> - *Radiolytic decomposition of ion exchange resins to produce gaseous products in alkaline media is well studied.*
> - *Organic backbone type resin degradation fragments exist in SRS waste.*
> - *The authors found no literature evidence of VOC generation from thermolysis reactions.*

Technical specification sheets from vendors for ion exchange resins[80,81] state that recommended operating

temperatures can be as high as 250 °C for cation exchangers and 100 °C to 120 °C for weak and strong anion exchangers, respectively, in raw water applications per Miller's SUEZ Water Technologies Report 'TP1050EN'.[80] The Dow Chemical information[81] shows loss of resin capacity of ~ 20% at 80 °C, declining sharply to around 75% capacity loss at 100° C. The chemical mechanism suggested by Dow Chemical for the thermal degradation of basic anion exchange resins involves either formation of methanol by reaction pathway (1) or trimethylamine by reaction pathway (2), as shown in Figure 2-16. Both mechanisms can be postulated as attack by the hydroxide anions (OH⁻) on either one of the methyl groups resulting in pathway (1), or attack on the R-CH$_2$-N carbon resulting in R-CH$_2$OH and trimethylamine in pathway (2). Neither of these postulated routes would produce a free methyl radical (•CH$_3$) that could subsequently produce hydrogen or methane by Equations 2-5.
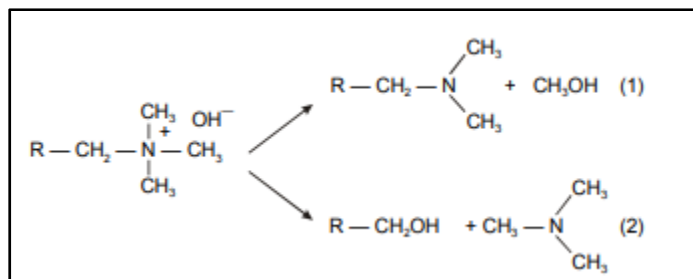

Figure 2-16. Thermal Degradation Pathways for Basic Anion Exchange Resin

Current thermolysis testing will use oxidized compounds to mimic fragments of styrene/divinylbenzene copolymer resins to access hydrogen generation rates.[38] The three aromatic compounds chosen for study are benzendicarboxylic acid, methylcarboxylpyridinium and sulfobenzoic acid. Only one of these species (methylcarboxylpyridinium) contains an end member methyl group.

3.0 Conclusions

The 2017 report *Flammable Gas Generation Mechanisms for High Level Liquid Waste Facilities*, X-ESR-G-00062 Rev. 1, assessing mechanisms for flammable gas generation acknowledged the presence of flammable organics, concluding that available data indicated their concentrations pose a minor contribution (e.g., <5%) to the composite lower flammable limit. SRR chartered the SRNL to perform a more detailed assessment of available and emerging data to assess the current state of knowledge for formation of VOCs from thermolysis of organics in SRS caustic tank waste.

Based on the assessment as detailed herein, SRNL concludes that sufficient evidence exists to demonstrate formation of methane, in addition to hydrogen, does occur during thermolysis of SRS high level waste containing organics under select conditions. This assessment cannot reliably quantify the amount of methane that forms. Nevertheless, the potential rates are sufficient – methane generation rates of approximately 30% and 100% those of hydrogen generation rates for Tank 38 radioactive waste and a HBP simulant waste, respectively – to advise that ongoing program efforts be enhanced to include additional analysis for off-gas generation for concentration and screening measurements for other possible flammable species. The following paragraphs provide summary statements for the individual lines of inquiry that support this conclusion followed by a list of recommendations for the options of enhanced measurements.

- Review of recent SRS waste tank vapor sampling specific to IH related hazardous components shows concentrations of numerous VOCs fell below the detection limits. These data have been compared to radiolytic HGRs from CSTF tanks to show that none of the VOCs at their detection limit concentrations would contribute more than 5% of the total hydrogen flammability per *Determination of the*

Flammability Ratio of Hydrogen Gas to Volatile Organic Carbons, X-CLC-H-01225. In addition, the sampling program did not measure for the presence of methane, which is an expected species.

- Review of published data and reports from the Hanford Site yields the following key observations.

  o Testing with both simulated and actual Hanford Site high-level waste samples provides evidence of methane from thermolysis.
  o Testing shows the methane-to-hydrogen ratio increases with temperature, going from <0.05 at 60 °C, in the range of 0.21 to 0.42 for 90 °C and approaching values of between 0.5 (for 66 hour tests) and 1 (for 207 hour tests) at 120 °C. Ammonia concentrations relative to hydrogen increase from none detected at 60 °C to 90 °C, to ~3-4% at 120 °C with C_2 hydrocarbon (ethane, ethylene or acetylene) concentrations still less than 1% that of hydrogen.
  o HGRs decrease in going from 20% oxygenated to inert atmospheres for high TOC Hanford samples, whereas methane rates are less affected, which may result in higher methane-to-hydrogen ratios in inert systems vs. the 20% oxygenated tests.
  o The Hanford Site high-level waste program uses a 10% of overall HGR as the bounding contribution for methane. Since the HGR is dependent on salt concentration, dose rate, temperature, TOC and aluminum concentrations, the methane generation rate fluctuates accordingly. This approach is in contrast to the fixed 5% of hydrogen LFL that SRS uses for contribution from all VOCs.

- Given the recent and emerging SRNL experimental data from thermolysis of SRS simulated and actual waste reported in *Investigation of Thermolytic Hydrogen Generation Rate of Tank Farm Simulated and Actual Waste* (SRNL-STI-2017-00611, Rev. 0), it is demonstrated that VOC generation by thermolysis, like that documented by Hanford studies cited in this report, could occur with SRS waste containing organics.

- The report on thermolysis testing of an actual SRS waste sample reported in *Investigation of Thermolytic Hydrogen Generation Rate of Tank Farm Simulated and Actual Waste* (SRNL-STI-2017-00611 Rev. 0) identified three unknown chromatograph peaks. Subsequent (and ongoing) analysis identified one peak as methane with the other two suspected as anomalous features. Preliminary estimates place the relative concentration of methane to hydrogen at ~30-35% for Tank 38 waste at boiling although the data is too sparse and too close to detection limits to provide a fully reliable value. The unknown chromatograph peak from simulant testing was also subsequently identified as methane. The simulant used conservative concentrations of multiple organics not likely to be present concurrently in a single waste feed. Preliminary estimates indicate equivalent concentrations of methane and hydrogen in the simulated waste tests that used high concentrations of the organics found in SRS waste.

- Presence of organo-mercury compounds may provide a route to methane formation, but confirmatory evidence is lacking for the waste matrix. Currently, the authors have not ascertained conclusive evidence of methane formation at SRS waste storage and processing conditions. The authors use recent data on stability of dimethyl mercury, which has been analyzed to be ~ 1 mg/L in some SRS CSTF tanks to provide an order of magnitude estimate of the potential generation rate for methane (e.g., methane generation rates of 9.1E-09 to 2.0E-06 ft^3/gal·hr in the temperature range of 39 to 170 °C in a HLW simulant) for comparison purposes. Unfortunately, the authors have not yet located sufficient data on methyl mercury, present at levels up to ~ 200 mg/L in SRS CSTF tanks, to allow estimating the methane generation rate for that compound in alkaline solution. However, an estimated methane generation in reagent water is provided (e.g., methane generation rates of 2.2E-07 to 4.5E-02 ft^3/gal·hr in the temperature range of 26 to 170 °C).

SRNL-STI-2018-00163
Revision 1

- Methane formation in the Bayer process from thermolysis tends to show a hydrogen-to-methane molar ratio of ≥75 (albeit at temperatures significantly higher than SRS waste processing conditions).

- Published studies of processing liquids obtained from the Bayer process cited in this report (from 2011 to 2016), albeit at more extreme conditions (175 °C to 275 °C), with a wide range of compounds, provide insight into the relative stability of classes of compounds toward hydrogen formation. By extrapolation and comparison to organics in SRS waste, antifoam is expected to show higher propensity for hydrogen (or flammable gas) formation. Ion exchange resins and solvents, in decreasing order, will likely yield lower quantities per unit mass of starting organic.

- Combined thermolysis and radiolysis studies for the cesium removal solvent suggest a potential methane-to-hydrogen ratio near ~0.24 with lesser amounts of other VOCs after long irradiation times. This magnitude agrees reasonably well with radiolysis data for PUREX solvent.

- Prior testing on off-gas production from thermolysis or radiolysis of antifoam does not provide insight into whether lighter VOCs formed. Preliminary findings from current SRNL HGR testing indicates that methane is produced at ~10X the rate as hydrogen from 100 °C thermolysis testing of the antifoam degradation product trimethylsilanol in a Tank 38 simulant.

- Decomposition of TBP and the degradation products in alkaline media is well studied. The authors found no literature evidence of methane generation from the TBP reaction system.

- Radiolytic decomposition of ion exchange resins to produce gaseous products in alkaline media is well studied. Degradation fragments from the organic backbone of resins exist in SRS waste. The authors found no literature evidence of VOC generation from thermolysis reactions involving these compounds. However, the absence of data may be a limitation of the prior testing focusing on hydrogen production and should not be construed as evidence that VOCs do not form.

4.0 Recommendations

1. Considering this assessment, SRNL recommends pursuing additional steps in ongoing and future experimental work to measure the presence of flammable VOCs in the thermolysis studies.

   e) In SRNL experiments, employ readily available gas analysis instrumentation (such as FTIR spectroscopy coupled with MS) capable of quantifying simple VOCs such as methane, ethane/ethylene and other low carbon containing gaseous flammable hydrocarbons. Use this equipment first in experiments involving simulated waste to most quickly provide additional information on species present and approximate concentration ranges. Based on those findings, determine whether deployment with radioactive waste samples is warranted.
   f) Assess the option of altering the SRNL GC protocols for (a) longer duration sampling capable of detecting at least ethane and possible C3 compounds on the second column used in the current GC system. In addition, consider (b) altering the carrier gas configuration to the second column within the GC to enhance sensitivity for analysis of these compounds. If the method appears viable, aggressively pursue implementation of these options in tests for both simulated and actual waste studies. Deploy these changes at the earliest practical date.
   g) Expand the available calibration gases for additional VOCs. By practical necessity and for expedient progress in understanding, these procurements should proceed in parallel with the

previous two recommendations but not preclude development and testing of the alternate analytical protocols.

h) Charter a Technical Agency to develop costs estimates and options for enhanced analytical methods for VOCs in the off-gas from future test programs and to enhance organic compound identification in high level waste samples.

2. A Technical Agency should conduct a review of prior sludge batch qualification off-gas analysis data for additional data related to presence of lighter VOCs other than the known ADPs. Similar reviews should occur of any archived data files for CSTF related off-gas studies that may also contain evidence of VOCs not previously identified.

3. If the review of prior sludge batch qualification off-gas analysis data shows presence of lighter VOCs, then SRR should consider requesting a Technical Agency to adopt similar expansion in analytical options for sludge batch qualification studies (i.e., actual waste sample testing) planned for the DWPF.

4. SRR should reassess the current assumption that VOCs provide a bounding 5% contribution to composite flammable limit beyond that of hydrogen with emphasis on applications involving increased temperatures where thermolysis reactions could produce VOCs with generation rates of the same order of magnitude as HGRs produced by radiolysis or thermolysis.

5. SRR should consider including other VOCs such as methane, ethane and ethylene measurements in Industrial Hygiene sensitive volatile compounds from CSTF vapor sampling to provide information on these species with respect to possible flammability concerns.

6. SRR should consider requesting SRNL to perform thermolysis studies to investigate degradation of methylmercury to form hydrogen and VOCs in an alkaline aqueous waste matrix in addition to ongoing HGR studies involving prominent organics in SRS waste.

7. Revise the previous technical report on the thermolysis study of SRNL simulant and radioactive Tank 38 samples presented in *Investigation of Thermolytic Hydrogen Generation Rate of Tank Farm Simulated and Actual Waste* (SRNL-STI-2017-00611 Rev. 0) to include further treatment of the 'unknown' peaks identified in that work (that is presented in this study).

5.0 References

1. Martino, C. J.; Woodham, W. H.; McCabe, D. J.; Nash, C. A. *Task Technical and Quality Assurance Plan for Simulant and Radioactive Testing of the Impacts of Glycolate on Hydrogen Generation in the Savannah River Site Liquid Waste System*; SRNL-RP-2017-00684, Rev. 1; 2018.

2. Clark, M. C. *Simulant and Radioactive Tesing - Impact of Glycolate on Tank Farms*; X-TTR-S-00067, Rev. 2; 2018.

3. Keilers, C. H., Jr; Altman, S. N.; Crawford, C. L.; Fink, S. D.; Henley, D.; Mills, J.; Wiersma, B. J. *Flammable Gas Generation Mechanisms for High Level Liquid Waste Facilities*; X-ESR-G-00062, Rev. 1; 2017.

4. Martino, C. J.; Newell, J. D.; Woodham, W. H.; Pareizs, J. M.; Edwards, T. B.; Lambert, D. P.; Howe, A. M. *Investigation of Thermolytic Hydrogen Generation Rate of Tank Farm Simulated and Actual Waste*; SRNL-STI-2017-00611, Rev. 0; 2017.

5. Walker, D. D. *Organic Compounds in Savannah River Site High-Level Waste*; WSRC-TR-2002-00391, Rev. 0; 2002.

6. Hobbs, D. T. *Possible Explosive Compounds in the Savahhan River Site Waste Tank Farm Facilities*; WSRC-TR-91-444, Rev. 3; 2000.

7. Britt, T. E. *Resolution of the Organic PISA*; WSRC-TR-2002-00094, Rev. 3; 2003.

8. Swingle, R. F. *Organic PISA Table Top Review for Miscellaneous Organic Compounds in the Tank Farm*; SRT-LWP-99-00081; 1999.

9. Costine, A.; Loh, J. S. C.; Power, G.; Schibeci, M.; McDonald, R. G. Understanding Hydrogen in Bayer Process Emissions. 1. Hydrogen Production during the Degradation of Hydroxycarboxylic Acids in Sodium Hydroxide Solutions. *Ind. Eng. Chem. Res.* 2011, *50* (22), 12324-12333.

10. Costine, A.; Loh, J. S. C.; Power, G. Understanding Hydrogen in Bayer Process Emissions. 2. Hydrogen Production during the Degradation of Unsaturated Carboxylic Acids in Sodium Hydroxide Solutions. *Ind. Eng. Chem. Res.* **REQUIRED TRANSFER DATA FOR M016228** *50* (22), 12334-12342.

11. Costine, A.; Loh, J. S. C.; Busetti, F.; Joll, C. A.; Heitz, A. Understanding Hydrogen in Bayer Process Emissions. 3. Hydrogen Production during the Degradation of Polyols in Sodium Hydroxide Solutions. *Ind. Eng. Chem. Res.* 2013, *52* (16), 5572-5581.

12. Costine, A.; Loh, J. S. C. Understanding Hydrogen in Bayer Process Emissions. 4. Hydrogen Production during the Wet Oxidation of Industrial Bayer Liquor. *Ind. Eng. Chem. Res.* 2016, *55* (16), 4415-4425.

13. Staub, A. V. *Potentially Inadequate Recognition of the Effect of Organics on Hydrogen Generation Rates in Saltstone*; PI-2017-0002; 2017.

14. Condon, W. A. *Potentially Inadequate Recognition of the Effect of Organics on Hydrogen Generation Rates in CSTF*; PI-2017-0003; February 28, 2017.

15. Brotherton, K. M. *Potentially Inadequate Recognition of the Effect of Organics on Hydrogen Gas Generation Rates in DWPF Process Vessels*; PI-2017-0004; February 28, 2017.

16. Clare, A. T. *Evaluation of the Saltstone Controls Considering the Inclusion of Organic Contribution to Radiolytic and Thermolytic Hydrogen Generation*; X-ESR-Z-00037, Rev. 0; 2017.

17. Clare, A. T. *Inclusion of Organic Contribution to Radiolytic and Thermolytic Hydrogen Generation at DWPF*; X-ESR-S-00320, Rev. 2; 2017.

18. Guardiano, S. K. *Inclusion of Organic Contribution to Radiolytic and Thermolytic Hydrogen Generation at CSTF*; X-ESR-G-00061, Rev. 0; 2017.

19. Ray, J. W. *Waste Acceptance Criteria for Aqueous Waste Sent to the Z-Area Saltstone Production Facility*; X-SD-Z-00001, Rev. 17; 2017.

20. Arnold, J. P. *Waste Acceptance Criteria for Liquid Waste Transfers to the Tank Farms (U)*; X-SD-G-00001, Rev. 41; 2018.

21. Wilmarth, W. R.; Maier, M. A.; Armstrong, T. W.; Ferry, R. L.; Henshaw, J. L.; Holland, R. A.; Jayjock, M. A.; Le, M. H.; Rock, J. C.; Timchalk, C. *Hanford Tank Vapor Assessment Report*; SRNL-RP-2014-00791, Rev. 0; 2014.

22. Thaxton, G. D.; Bumgardner, D. C.; Kahal, E. J.; Schweder, M. B.; Stoyle, C. B.; Wilmarth, W. R. *Review of Hanford Tank Vapor Assessment Team Recommendations for Applicability to Savannah River Remediation*; SRR-LWE-2015-00050, Rev. 0; 2015.

23. Thaxton, G. D.; Bumgardner, D. C.; Kahal, E. J.; Schweder, M. B. *Savannah River Remediation Tank Vapor Action Plan*; SRR-ESH-2015-00090, Rev. 0; 2015.

24. Schweder, M. B. *SRS Tank Vapor Sampling Plan*; SRR-FSH-2015-00026, Rev. 0; 2004, 2015.

25. Barrowclough, E. P. *Determination of the Flammability Ratio of Hydrogen Gas to Volatile Organic Carbons*; X-CLC-H-01225, Rev. 0; 2017.

26. Barrowclough, E. P. *Savannah River Remediation Tank Vapor Report*; X-ESR-H-00938, Rev. 0; 2018.

27. Ashley, K.; O'Connor, F., *NIOSH Manual of Analytical Methods (NMAM) 5th Edition*. 2017.

28. Chew, D. *Savannah River Site - Waste Tank Levels*; SRR-LWP-2010-00001, Rev. 58; 2017.

29. Bui, H. *CSTF Flammability Control Program - Program Description Document*; WSRC-TR-2003-00087, Rev. 32; 2018.

30. Patel, N. P., McKibbin, B. A. *Evaluation of the Safety of the Situation (ESS): Potentially Inadequate Recognition of the Effect of Organics on Hydrogen Generation Rates in the Concentration, Storage, and Transfer Facilities (PISA PI-2017-0003)*; U-ESS-G-00007, Rev. 2; 2018.

31. Hu, T. A. *Empirical Rate Equation Model and Rate Calculations of Hydrogen Generation for Hanford Tank Waste*; HNF-3851, Rev. 1; 2004.

32. Bryan, S. A.; Camaioni, D. M.; Levitskaia, T. G.; McNamara, B. K.; Sell, R. L.; Stock, L. M. *Gas Generation Testing and Support for the Hanford Waste Treatment and Immobilization Plant*; PNWD-3463, WTP-RPT-115, Rev. 0; 2004.

33. King, C. M.; Bryant, S. A. *Thermal and Radiolytic Gas Generation Tests on Material from Tanks 241-U-103, 241-AW-101, 241-S-106, and 241-S-102: Status Report*; PNNL-12181, UC-2030; 1999.

34. Pederson, L. R., Bryan, S. A. *Status and Integration of Studies of Gas Generation in Hanford Wastes*; PNNL-11297, UC-2030; 1996.

35. Ashby, E. C.; Annis, A.; Barefield, E. K.; Boatright, D.; Doctorovich, F.; Liotta, C. L.; Neumann, H. M.; Konda, A.; C.F., Y.; Zhang, K.; McDuffie, N. G. *Synthetic Waste Chemical Mechanism Studies*; WHC-EP-0823, Rev. 0; 1994.

36. Yarbrough, R. J. *Steady-State Flammable Gas Release Rate Calculation and Lower Flammability Level Evaluation for Hanford Tank Waste*; RPP-5926, Rev. 17; 2016.

37. Stock, L. M. *Occurrence and Chemistry of Organic Compounds in Hanford Site Waste Tanks*; RPP-21854, Rev. 0; 2004.

38. Woodham, W. H. *Run Plan for Testing to Screen and Assess the Hydrogen Generation Rates Evolved from the Thermolysis of Glycolate and Other Prominent Tank Farm Organics*; SRNL-L3300-2018-00004, Rev. 0; 2018.

39. Reboul, S. H.; Newell, J. D.; Pareizs, J. M.; Coleman, C. J. *Low Temperature Aluminum Dissolution (LTAD) Real Waste Testing of the November 2017 Tank 51 Slurry Sample*; SRNL-STI-2018-00179, Rev. 0; 2018.

40. Bannochie, C. J. *Results of Hg Speciation Testing on the 3Q17 Tank 50 Sample*; SRNL-L3300-2017-00037, Rev. 1; 2018.

41. Jain, V.; Shah, H. B.; Occhipinti, J. E.; Wilmarth, W. R.; Edwards, R. E. *Evaluation of Mercury in Liquid Waste Processing Facilities Phase I Report*; SRR-CES-2015-00012, Rev. 1; 2015.

42. Banochie, C. J.; Fellinger, T. L.; Garcia-Strickland, P.; Shah, H. B.; Jain, V.; Wilmarth, W. R. Mercury in Aqueous Tank Waste at the Savannah River Site: Facts, Forms and Impacts. http://dx.doi.org/10.1080/01496395.2017.1310239.

43. Jain, V.; Shah, H. B.; Occhipinti, J. E.; Wilmarth, W. R.; Edwards, R. E. *Evaluation of Mercury in Liquid Waste Processing Facilities – Comprehensive Action Plan for the Long-Term Management and Removal of Mercury in the Savannah River Site Liquid Waste System*; SRR-CES-2016-00026, Rev. 0; 2016.

44. Bannochie, C. J.; Crawford, C. L.; Jackson, D. G.; Shah, H. B.; Jain, V.; Occhipinti, J. E.; Wilmarth, W. R. *Mercury Phase II Study – Mercury Behavior across the High-Level Waste Evaporator System*; SRNL-STI-2016-00163, Rev. 0; 2016.

45. Wilmarth, W. R. *Frontier Formation Report*; SRNL-WHM-2004-00009, Rev. 0; 2004.

46. Kozin, L. F.; Hansen, S. C., *Mercury Handbook: Chemistry, Applications and Environmental Impact*. Royal Society of Chemistry: 2013.

47. Parker, J. L.; Bloom, N. S. Preservation and Storage Techniques for Low-level Aqueous Mercury Speciation. *Science of the Total Environment* 2005**,** *337* (1-3), 253-263.

48. Oremland, R. S.; Culbertson, C. W.; Winfrey, M. R. Methylmercury Decomposition in Sediments and Bacterial Cultures: Involvment of Methanogens and Sulfate Reducers in Oxidative Demethylation. *Applied and Environmental Microbiology* 1991, *57* (1), 130-137.

49. Jeremiason, J. D.; Portner, J. C.; Aiken, G. R.; Hiranaka, A. J.; Dvorak, M. T.; Tran, K. T.; Latch, D. E. Photoreduction of Hg(II) and Photodemethylation of Methylmercury: The Key Role of Thiol Sites on Dissolved Organic Matter. *Environ. Sci. : Processes & Impacts* 2015, *17* (11), 1892-1903.

50. Leopold, K.; Foulkes, M.; Worsfold, P. Methods for the Determination and Speciation of Mercry in Natural Waters - A Review. *Analytical Chimica Acta* 2010, *663* (2), 127-138.

51. Ebadian, M. A. *Mercury Contaminated Material, Decontamination Methods: Investigation and Assessment*; HCET-2000-D053-002-04; 2001.

52. Abranko, L.; Jokai, Z.; Fodor, P. Investigation of the Species-specific Degradation Behavior of Methylmercury and Ethylmercury under Microwave Irradiation. *Anal. Bioanal. Chem.* 2005**,** *383* (3), 448-453.

53. Cotton, A. F., Wilkinson, G., *Advanced Inorganic Chemistry: A Comprehensive Text*. 4th ed.; John Wiley & Sons, Inc.: 1980.

54. Rabenstein, D. L. The Aqueous Solution Chemistry of Methylmercury and its Complexes. *Acc. Chem. Res.* 1978, *11* (3), 100-107.

55. Wilmarth, W. R. *Results of Dimethylmercury Degradation Experiments at Frontier Geosciences*; SRT-LWP-2004-00018; 2004.

56. Harvey, S. E. Stability of Monomethylmercury in Water. Electronic Masters Thesis, Wright State University, 2015.

57. Crawford, C. L.; King, W. D. *Impacts of Glycolate and Formate Radiolysis and Thermolysis on Hydrogen Generation Rate Calculations for the Savannah River Site Tank Farm*; SRNL-STI-2017-00303, Rev. 0; 2017.

58. Moyer, B. A.; Alexandratos, S. D.; Bonnesen, P. V.; Brown, G. M.; Caton, J. E.; Delmau, L. H.; Duchemin, C. R.; Haverlock, T. J.; Levitskaia, T. G.; Maskarinec, M. P.; Sloop, F. V.; Stine, C. L. *Caustic-Side Solvent Extraction Chemical and Physical Properties Progress in FY 2000 and FY 2001*; ORNL/TM-2001/285; 2002.

59. Roach, B. D.; Willams, N. J.; Moyer, B. A. Thermal Degradation of the Solvent Employed in the Next-Generation Caustic Solvent Extraction Process and Its Effect on the Extraction, Scrubbing, and Stripping of Cesium. *Solvent Extraction and Ion Exchange* 2015**,** *33* (6), 576-591.

60. Roach, B. D.; Willams, N. J.; Duncan, N. C.; Delmau, L. H.; Lee, D. L.; Birdwell, J. F.; Moyer, B. A. Radiolytic Treatment of the Next-Generation Caustic-Side Solvent Extraction (NGS) Solvent and Its Effect on the NGS Process. *Solvent Extraction and Ion Exchange* 2015**,** *33* (2), 134-151.

61. Moyer, B. A.; Birdwell, J. F.; Bonnesen, P. V.; Bruffey, S. H.; Delmau, L. H.; Duncan, N. C.; Ensor, D. D.; Hill, T. G.; Lee, D. L.; Rajbanshi, A.; Roach, B. D.; Szczygiel, P. L.; Sloop, F. V.; Stoner, E. L.; Willams, N. J. *Next Generation Solvent Development for Caustic-Side Solvent Extraction of Cesium*; ORNL/TM-2014/22; 2014.

62. Williams, N. J.; Roach, B. D.; Moyer, B. A.; Lee, D. L. *Next Generation CSSX Program Effect of Radiolytic and Thermal Treatment on the Performance of the Next-Generation Caustic-Side Solvent Extraction (NG-CSSX) Solvent*; ORNL-LTR-NGCSSX-017; 2011.

63. Mincher, B. *CSSX Radiolytic H_2 Generation ("Thermolysis") Final Report*; INL/EXT-09-15302, Rev. 0; 2009.

64. Bonnesen, P. V.; Del Cul, G. D.; Hunt, R. D.; Ilgner, R. H.; Tomkins, B. A. *Radiolysis of CSSX Solvents for Parsons Infrastructure & Technology Group in FY 2007 in Support of the Salt Waste Processing Facility at the Savannah River Site*; ORNL/TM-2007/093; 2007.

65. Poirier, M. R., Pareizs, J. M., Peters, T. B., Fink, S. D *SWPF Radiolysis and Thermolysis Test*; SRNL-STI-2009-00127, Rev. 0; 2009.

66. Aponte, C. I. *Qualification of Oak Ridge National Laboratory (ORNL) Next Generation Solvent (NGS) Test Data*; U-DQR-H-00001, Rev. 1; 2013.

67. Davis, W., Jr., *Science and Technology of Tributyl Phosphate*. CRC Press, Inc.: Boca Raton, Florida, 1984; Vol. 1.

68. White, T. L.; Wiedenman, B. J.; Lambert, D. P.; Crump, S. L.; Fondeur, F. F.; Papathanassiu, A. E.; Kot, W. K.; Pegg, I. L. *Organics Characterization of DWPF Alternative Reductant Simulants, Glycolic Acid, and Antifoam 747*; SRNL-STI-2013-00491, Rev. 0; 2013.

69. Zamecnik, J. R.; Newell, J. D. *Antifoam Degradation in the DWPF Chemical Process Cell*; SRNL-L3100-2015-00088, Rev. 0; 2015.

70. Lambert, D. P.; Zamecnik, J. R.; Newell, J. D.; Williams, M. S. *Antifoam Degradation Testing*; SRNL-STI-2015-00352, Rev. 0; 2015.

71. Hay, M. S.; Martino, C. J. *Analysis of Condensate Samples in Support of the Antifoam Degradation Study*; SRNL-STI-2015-00698, Rev. 1; 2016.

72. Martino, C. J.; Crawford, C. L. *Results of Antifoam Degradation Product Analysis of Tank 22H*; SRNL-L3100-2015-00146, Rev. 0; 2015.

73. Smith, T. E. *Antifoam Degradation Products in Off Gas and Condensate of Sludge Batch 9 Simulant Nitric-Formic Flowsheet Testing for the Defense Waste Processing Facility*; SRNL-STI-2016-00110, Rev. 0; 2016.

74. Brandys, M.; Penafiel, M.; Abramowitz, H.; Pegg, I. L. *Final Report DWPF Antifoam Degradation Product Testing*; VSL-16R4200-1, Rev. 0; 2016.

75. Lambert, D. P.; Willams, M. S.; Brandenburg, C. H.; Luther, M. C.; Newell, J. D.; Woodham, W. H. *Sludge Batch 9 Simulant Runs Using the Nitric-Glycolic Acid Flowsheet*; SRNL-STI-2016-00319, Rev. 0; 2016.

76. Campbell, J. A.; Hoppe, E. W.; Greenwood, L. R.; Farmer, O. T. *Organic and Actinide Characterization of SRS Tank Waste Samples Subtask C*; PNNL-14039, Rev. 0; 2003.

77. Stallings, M. E.; Barnes, M. J.; Peters, T. B.; DiPrete, D. P.; Fondeur, F. F.; Hobbs, D. T.; Fink, S. D. *Characterization of Supernate Samples from High Level Waste Tanks 13H, 30H, 37H, 39H, 45F, 46F and 49H*; WSRC-TR-2004-00386, Rev. 2; 2005.

78. Swingle, R. F.; Poirier, M. R. *Tank Farm Organic PISA Study Final Report*; WSRC-TR-99-00333, Rev. 1; 2000.

79. Britt, T. E. *Location of the Principal Volatile Organics, Ammonia Compounds, Organo-Metallics, and NOx Gases Resident in the Tank Farm*; X-ESR-H-00020, Rev. 0; 2004.

80. Miller, W. S.; Castagna, C. J.; Pieper, A. W. Understanding Ion-Exchange Resins for Water Treatment Systems; TP1050EN.docx; SUEZ Water Technologies & Solutions; 2017,. www.suezwatertechnologies.com.

81. Temperature Stability of Anion Exchange Resins; 177-017501, Rev. 0; DOW; 2016,. http://msdssearch.dow.com/PublishedLiteratureDOWCOM/dh_0999/0901b80380999021.pdf?filepath=liquidseps/pdfs/noreg/177-01751.pdf&fromPage=GetDoc.

Appendix A. Supplemental Information from Bayer Process Thermolysis Studies

Table A-1. Table of Organic Compounds for Thermolysis Testing from Reference [9].

Table 1. Aliphatic and Aromatic Compounds Used in the Current Work

compound	structure
formate	$H \cdot CO_2^-$
acetate	$CH_3 \cdot CO_2^-$
propanoate	$CH_3 \cdot CH_2 \cdot CO_2^-$
butanoate	$CH_3 \cdot (CH_2)_2 \cdot CO_2^-$
valerate	$CH_3 \cdot (CH_2)_3 \cdot CO_2^-$
caproate	$CH_3 \cdot (CH_2)_4 \cdot CO_2^-$
heptanoate	$CH_3 \cdot (CH_2)_5 \cdot CO_2^-$
isobutyrate	$(CH_3)_2 \cdot CH \cdot CO_2^-$
oxalate	$CO_2^- \cdot CO_2^-$
malonate	$CO_2^- \cdot CH_2 \cdot CO_2^-$
succinate	$CO_2^- \cdot (CH_2)_2 \cdot CO_2^-$
glutarate	$CO_2^- \cdot (CH_2)_3 \cdot CO_2^-$
tricarballylate	$CO_2^- \cdot CH_2.CH(CO_2^-) \cdot CH_2.CO_2^-$
benzoate	$C_6H_5 \cdot CO_2^-$
phthalate (1,2-benzenedicarboxylate)	$C_6H_4 \cdot (CO_2^-)_2$
isophthalate (1,3-benzenedicarboxylate)	$C_6H_4 \cdot (CO_2^-)_2$
terephthalate (1,4-benzenedicarboxylate)	$C_6H_4 \cdot (CO_2^-)_2$
trimellitate (1,2,4-benzenetricarboxylate)	$C_6H_3 \cdot (CO_2^-)_3$
trimesate (1,3,5-benzenetricarboxylate)	$C_6H_3 \cdot (CO_2^-)_3$
pyromellitate (1,2,4,5-benzenetetracarboxylate)	$C_6H_2 \cdot (CO_2^-)_4$
glycolate	$CH_2(OH) \cdot CO_2^-$
lactate	$CH_3 \cdot CH(OH) \cdot CO_2^-$
2-hydroxybutanoate	$CH_3 \cdot CH_2 \cdot CH(OH) \cdot CO_2^-$
3-hydroxybutanoate	$CH_3 \cdot CH(OH) \cdot CH_2 \cdot CO_2^-$
malate	$CO_2^- \cdot CH(OH) \cdot CH_2 \cdot CO_2^-$
D-tartrate	$CO_2^- \cdot (CH(OH))_2 \cdot CO_2^-$
L-tartrate	$CO_2^- \cdot (CH(OH))_2 \cdot CO_2^-$
meso-tartrate	$CO_2^- \cdot (CH(OH))_2 \cdot CO_2^-$
ribonate	$CH_2(OH) \cdot (CH(OH))_3 \cdot CO_2^-$
galactarate	$CO_2^- \cdot (CH(OH))_4 \cdot CO_2^-$
citrate	$CO_2^- \cdot CH_2 \cdot C(CO_2^-)(OH) \cdot CH_2 \cdot CO_2^-$
gluconate	$CH_2(OH) \cdot (CH(OH))_4 \cdot CO_2^-$
16-hydroxyhexadecanoate	$CH_2(OH) \cdot (CH_2)_{14} \cdot CO_2^-$
catechol (1,2-dihydroxybenzene)	$C_6H_4 \cdot (OH)_2$
resorcinol (1,3-dihydroxybenzene)	$C_6H_4 \cdot (OH)_2$
salicylate (2-hydroxybenzoate)	$CO_2^- \cdot C_6H_4 \cdot OH$
m-salicylate (3-hydroxybenzoate)	$CO_2^- \cdot C_6H_4 \cdot OH$
3,4-dihydroxybenzoate	$CO_2^- \cdot C_6H_3 \cdot (OH)_2$
pyrogallol (1,2,3-trihydroxybenzene)	$C_6H_3 \cdot (OH)_3$
gallate (3,4,5-trihydroxybenzoate)	$CO_2^- \cdot C_6H_2 \cdot (OH)_3$

Table A-2. Table of Organic Compounds for Thermolysis Testing from Reference [10].

Table 1. Unsaturated Compounds Used in the Current Work

compound	structure	refs[a]
		unsaturated monocarboxylates
acrylate	$CH_2=CH \cdot CO_2^-$	cellulose;[30] phenol;[31,32] pyridine;[33] succinic acid[34]
2-butenoate	$CH_3 \cdot CH=CH \cdot CO_2^-$	
3-butenoate	$CH_2=CH \cdot CH_2 \cdot CO_2^-$	
2-pentenoate	$CH_3 \cdot CH_2 \cdot CH=CH \cdot CO_2^-$	
2-hexenoate	$CH_3 \cdot (CH_2)_2 \cdot CH=CH \cdot CO_2^-$	
		unsaturated dicarboxylates
maleate (cis-butenedioate)	$CO_2^- \cdot CH=CH \cdot CO_2^-$	1,4-benzoquinone;[35,36] catechol, hydroquinone;[36] cellulose;[30] 2,6-dimethoxyphenol, 2-methoxyphenol;[37] 1,4-hydroxybenzoic acid;[35] phenol;[31,32,35−42] pyridine[33]
fumarate (trans-butenedioate)	$CO_2^- \cdot CH=CH \cdot CO_2^-$	1,4-benzoquinone, hydroquinone;[36] 2,6-dimethoxyphenol, 2-methoxyphenol;[37] phenol[31,32,36,37,39,41,42]
dihydroxyfumarate	$CO_2^- \cdot C(OH)=C(OH) \cdot CO_2^-$	
glutaconate	$CO_2^- \cdot CH_2 \cdot CH=CH \cdot CO_2^-$	2,6-dimethoxyphenol, 2-methoxyphenol, phenol;[37] pyridine[33]

[a] Parent compounds that produce unsaturated compounds (in their acidic forms) as intermediate products in wet oxidation studies.

Table A-3. **Table of Organic Compounds for Thermolysis Testing from Reference [11].**

Figure 1. Structures and Fischer projections of the polyols studied in which ω represents a primary hydroxyl−secondary hydroxyl sequence, "t" represents a threo sequence, and "e" represents an erythro sequence. The abbreviated hydroxyl sequences are written from the top carbon atom down.

Distribution:

timothy.brown@srnl.doe.gov
alex.cozzi@srnl.doe.gov
david.crowley@srnl.doe.gov
a.fellinger@srnl.doe.gov
samuel.fink@srnl.doe.gov
nancy.halverson@srnl.doe.gov
erich.hansen@srnl.doe.gov
connie.herman@srnl.doe.gov
john.mayer@srnl.doe.gov
daniel.mccabe@srnl.doe.gov
Gregg.Morgan@srnl.doe.gov
frank.pennebaker@srnl.doe.gov
William.Ramsey@SRNL.DOE.gov
luke.reid@srnl.doe.gov
geoffrey.smoland@srnl.doe.gov
michael.stone@srnl.doe.gov
Boyd.Wiedenman@srnl.doe.gov
bill.wilmarth@srnl.doe.gov
charles.crawford@srnl.doe.gov
charles.nash@srnl.doe.gov
john.pareizs@srnl.doe.gov
aaron.washington@srnl.doe.gov
chris.martino@srnl.doe.gov
Wesley.Woodham@srnl.doe.gov
dan.lambert@srnl.doe.gov
jeffrey.crenshaw@srs.gov
james.folk@srs.gov
roberto.gonzalez@srs.gov
tony.polk@srs.gov
patricia.suggs@srs.gov
Kevin.Brotherton@srs.gov
Richard.Edwards@srs.gov
terri.fellinger@srs.gov
eric.freed@srs.gov
jeffrey.gillam@srs.gov
barbara.hamm@srs.gov
bill.holtzscheiter@srs.gov
john.iaukea@srs.gov
Vijay.Jain@srs.gov
Victoria.Kmiec@srs.gov
jeff.ray@srs.gov
paul.ryan@srs.gov
Azadeh.Samadi-Dezfouli@srs.gov
hasmukh.shah@srs.gov
aaron.staub@srs.gov

Christie.sudduth@srs.gov
Jocelin.Stevens@srs.gov
Grace.Chen@srs.gov
Mason.Clark@srs.gov
hilary.bui@srs.gov
celia.aponte@srs.gov
timothy.baughman@srs.gov
earl.brass@srs.gov
Thomas.Huff@srs.gov
Christine.Ridgeway@srs.gov
arthur.wiggins@srs.gov
John.Occhipinti@srs.gov
Bill.Brasel@parsons.com
cliff.conner@parsons.com
Ryan.Lentsch@gat.com
Tom.Burns@parsons.com
Skip.Singer@parsons.com
Brad.Swanson@parsons.com
thomas.colleran@srs.gov
MARIA.RIOS-ARMSTRONG@SRS.GOV

Records Administration (EDWS)